STATE ESTIMATION OF UNBALANCED POWER SYSTEMS

by

Martin Wortman

Dissertation submitted to the Faculty of the

Virginia Polytechnic Institute and State University

in partial fulfillment of the requirements for the degree of

DOCTOR OF PHILOSOPHY

in

Electrical Engineering

APPROVED:

L. L. Grigsby, Chairman

A. G. Phadke

W. A. Blackwell

F. C. Brockhurst

C. L. Prather

August, 1982

Blacksburg, Virginia

ACKNOWLEDGMENTS

The author wishes to express his thanks to the many people at Virginia Tech who have given him encouragement and sound counsel for the past two and one-half years. Special appreciation is given to Dr. L. L. Grigsby, Chairman of the author's Advisory Committee, whose insight and teaching have made the author's graduate study a source of great satisfaction. Appreciation is also extended to the other members of the Advisory Committee, including Dr. W. A. Blackwell, Dr. F. C. Brockhurst, Dr. A. G. Phadke, and Dr. C. L. Prather.

Thanks are given to and for having provided many valuable suggestions. Appreciation is extended to , a fellow student and co-worker, for his collaboration in the modeling and analysis of unbalanced power systems.

Thanks are offered to the participants of the Energy Research Group; a research assistantship, offered through the ERG, has made the author's graduate study possible. Thanks are given to for typing the manuscript.

Finally, thanks are offered to , the author's wife, whose patience and understanding have been boundless.

TABLE OF CONTENTS

CHAPTER 1. INTRODUCTION

The static state of an electric power system is given as a vector of voltage magnitudes and angles from which all system steady state voltages can be determined. The static state estimator is a data processing algorithm which converts real-time meter readings into an estimate of the static state.

Power systems, due to continually changing load patterns, rarely achieve a true steady state operating point. It is, however, reasonable to assume that a power system operates in steady state over some short time interval. This quasi-steady state behavior suggests that a static state vector reflects the true system state. Hence, the static state will be referred to as the state and the static state estimator as the state estimator.

The available literature offers many results concerning the development of state estimators for balanced power systems [1-14]. These results address only those systems which can be accurately represented by a positive sequence network, principally high voltage bulk transmission networks.

Of increasing interest to the electric utility industry is real-time monitoring and control of lower voltage distribution networks. Such networks are, in general, characterized by topological imbalances, load imbalances, and a varying number of phases per line. Networks exhibiting these characteristics are referred to as unbalanced networks and cannot be accurately represented by a positive sequence network.

The results presented here offer a state estimation algorithm suitable for unbalanced power systems. The algorithm employs a deterministic network model which includes the effects of mutually coupled conductors, multiple grounding points, unbalanced transformer configurations, and earth return paths. Estimates of the state vector are in the phase-voltage reference frame.

1.1 Problem Statement

The power system state must be inferred from real-time meter readings telemetered from remote points throughout the system to some central location. These measurements are known to be noise corrupted and thus do not infer the true system state. The effects of measurement noise can be minimized by the introduction of a state estimator serving as a noise filter.

The most widely applied method of power system state estimation is the extended method of weighted least squares. This method requires that for a system of n state variables, there must be m measurements. Each measurement is equal to a real function of state variables only, yielding a set of m equations and n unknowns. The number of measurements m must be greater than the number of state variables n. Further, there must be n independent equations.

The measured variables are most often real and reactive conductor power flows, real and reactive loads, and phase voltage magnitudes. The state variables are most often phase voltage magnitudes and angles.

The power system state estimation problem can be stated as follows:

> Given m noise corrupted measurements (consist g of real and reactive conductor power flows, real and reac ve loads, and phase voltage magnitudes), determine the "bes estimate of the system state (n phase voltage magnitudes d angles) by the extended method of weighted least squares

In a real-time monitoring scenario, the state stimate must be updated periodically in order to closely approxima the true system state. The time interval over which a particular timate reasonably approximates the state is determined by the quasi-s ady state behavior of the given system.

1.2 State Estimation of Balanced Power Systems

The following key modeling considerations are mphasized with regard to state estimation of balanced power syste .

1) All systems are represented by a positive equence network.
2) All transformers can be represented as eq valent Π or T networks. All transformer banks are bala ed.
3) All lines are transposed and can be repre nted as equivalent Π networks.
4) The power system has common datum (ground node.

The above considerations suggest that the sys ms passive network (sources and loads excluded) can be modeled by Y_{BU} [15]. Thus, all sources and loads are connected at a common earth ound node and all phase voltages are referenced to this node.

For balanced networks, the state vector consi s of all phase voltage magnitudes and angles. Clearly, load meas ements are a function of Y_{BUS} and state variables only. Phase ltage magnitudes are a function of state variables only. Inasmuch as lines are represented by Π equivalent networks, complex conductor power flows can be obtained from Eq. (1.2.1). Here, S_{pq} is the complex flow from bus p to bus q as seen at bus p.

$$S_{pq} = V_p e^{j\delta_p} (V_p e^{-j\delta_p} - V_q e^{-j\delta_q})(G_{pq} - jB_{pq}) - jV_p^2 B_c \qquad (1.2.1)$$

Equation (1.2.1) follows directly from the Π line selection shown in Fig. 1.2.1.

The simplicity of conductor power flow calculations results from the absence of mutual coupling between elements of the equivalent Π section of Fig. 1.2.1.

1.3 Requirements for State Estimation of Unbalanced Power Systems

In contrast to state estimation of balanced power systems, the following modeling considerations are emphasized with regard to state estimation of unbalanced power systems.

1) Unbalanced systems cannot be represented by a positive sequence network. All system phases must be explicitly represented.
2) Transformer banks are generally unbalanced. Mutual coupling between phase windings can exist.
3) Lines and conductors are usually untransposed. Mutual coupling (inductive and capacitive) can exist. Lines cannot be represented as equivalent Π networks.
4) The earth's surface is a current path of nonzero resistivity. Thus, the power system can include many earth grounding points.

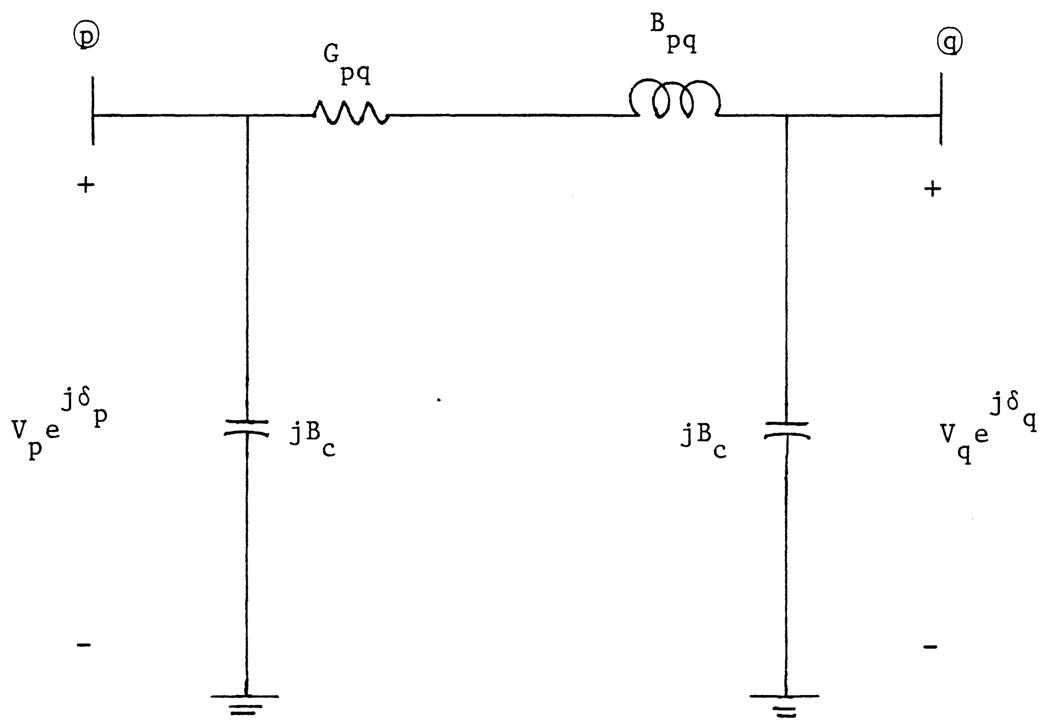

Fig. 1.2.1. Transmission line equivalent Π.

The above considerations suggest that the system's passive network (sources and loads excluded) cannot be modeled by Y_{BUS}. All phase voltages are referenced to a local neutral or a local ground node; line-to-line voltages of little practical interest.

Given the state estimation problem statement of Sec. 1.1, a model for unbalanced networks is required such that noise corrupted measurements are a function of state variables only. The results presented here offer such a model.

A method to systematically build an admittance matrix for unbalanced networks is developed. This admittance matrix exhibits the mathematical properties of Y_{BUS} and is applicable to both balanced and unbalanced networks.

The network admittance matrix is obtained from subnetwork admittance matrices. The network and subnetwork admittance matrices can be used to obtain load flow equations suitable for a state estimator.

Chapter 2 presents a general methodology for unbalanced network modeling. The general methodology is applied to both power subnetworks (segments) and networks. All admittance matrices are developed in the phase voltage reference frame.

Chapter 3 contains a development of state estimator equations for unbalanced power systems. The model of Chapter 2 is incorporated into the extended method of weighted least squares. The concept of port suppression is employed so that only nondeterministic measured variables are included in the estimator equations. The state estimator is demonstrated via simulation. Example simulations are offered for both balanced and unbalanced power systems.

CHAPTER 2. MULTIPORT NETWORK MODELING OF UNBALANCED POWER SYSTEMS

The network model offered in the sections to follow is intended to represent unbalanced power systems operating in steady state. The model yields a set of complex algebraic equations in variables convenient for state estimation.

The general methodology for obtaining multiport admittance matrices of passive networks is presented in Sec. 2.1. The correspondence between network ports and a given measurement tree is shown. Graph theoretic principles are used to obtain network multiport equations.

In Sec. 2.2, the general methodology is applied to obtain multiport equations of power system segments. Multiport equations are developed such that segment port variables correspond to system state and measured variables.

In Sec. 2.3, the general methodology is used to obtain multiport equations of power systems by interconnecting segment multiports. System equations yield port variables that correspond to measured variables. State variables established by the segment equations are retained.

Section 2.4 includes a discussion of linear dependence between port variables. The corresponding rank of multiport admittance matrices is considered. Normalization of multiport equations via an appropriate per-unitization scheme is discussed.

2.1 General Methodology

Development of the general methodology for obtaining multiport equations of passive networks appeals to linear graph theory. The following assumptions and definitions are necessary for a graph theoretic development.

<u>Assumptions and Definitions</u>

1) All networks are represented as directed graphs with spanning trees and cotrees defined.

   $\hat{t}$ = number of tree branches (twigs)

   $\hat{\ell}$ = number of cotree branches (links)

2) All network links represent linear passive admittances. Mutual admittance between links is permitted. Link current/voltage relationships (primitive equations) can be determined.

3) All network sources belong to the spanning tree (measurement tree). Sources need not be linear or independent. Dependent sources must be a function of twig variables.

4) A passive polarity convention is assumed for all branches.

   (a) current flow is directed as the branch arrow,

   (b) voltage polarity is such that the arrow is directed towards the negative branch terminal,

   (c) positive power indicates dissipation.

5) $A = [A_t \,|\, A_\ell]$, reduced node branch incidence matrix corresponding to a given tree. A_t = tree partition dimensioned $\hat{t} \times \hat{t}$; A_ℓ = cotree partition dimensioned $\hat{t} \times \hat{\ell}$.

6) $B = [B_t | U_\ell]$, fundamental loop matrix corresponding to a given tree. B_t = tree partition dimensioned $\hat{\ell} \times \hat{t}$; U_ℓ = identity matrix dimensioned $\hat{\ell} \times \hat{\ell}$.

7) $Q = [U_t | Q_\ell]$, fundamental cutset matrix corresponding to a given tree. U_t = identity matrix dimensioned $\hat{t} \times \hat{t}$; Q_ℓ = cotree partition dimensioned $\hat{t} \times \hat{\ell}$.

8) Branch voltage and current vectors are given by:

   (a) $\underline{V} = [\underline{V}_t^T | \underline{V}_\ell^T]^T$, voltage vector. $\underline{V}_t$ = tree partition; $\underline{V}_\ell$ = cotree partition.

   (b) $\underline{I} = [\underline{I}_t^T | \underline{I}_\ell^T]^T$, current vector. $\underline{I}_t$ = tree partition; $\underline{I}_\ell$ = cotree partition.

Any graph representing an electrical network must satisfy a set of topology (or network) constraints. Four (4) constraint equations, fundamental to development of the general methodology, are given below.

$$B\underline{V} = 0 \qquad (2.1.1)$$

$$Q\underline{I} = 0 \qquad (2.1.2)$$

$$QB^T = [0] \qquad (2.1.3)$$

$$AB^T = [0] \qquad (2.1.4)$$

Equations (2.1.1) and (2.1.2) are Kirchhoff's voltage and current laws. Equations (2.1.3) and (2.1.4) are properties of connected graphs.

Consider the arbitrary network shown in Fig. 2.1.1a. The network includes n nodes and b elements. There are s source elements and b-s admittance elements. Figure 2.1.1b shows the directed graph of the

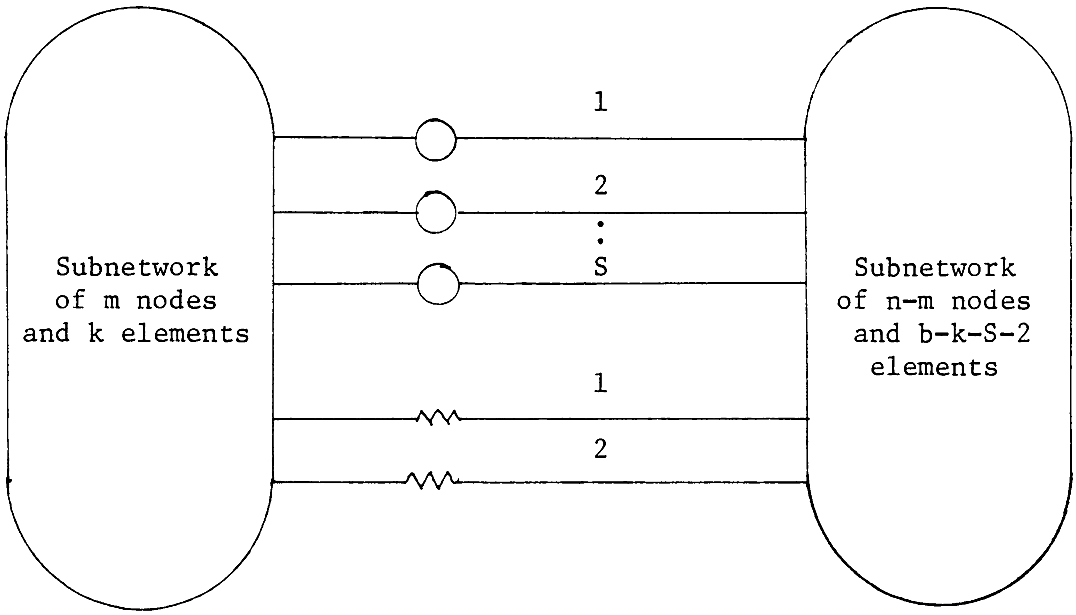

Fig. 2.1.1a. Arbitrary network of n nodes and b elements.

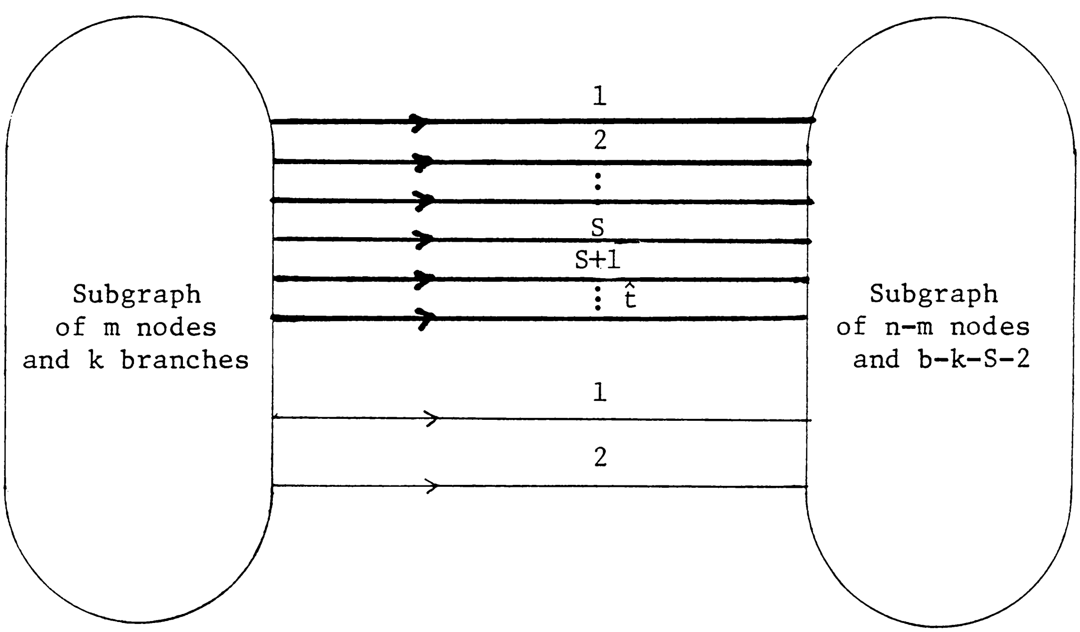

Fig. 2.1.1b. Directed graph corresponding to the arbitrary network.

given network. Darkened branches indicate twigs.

By definition, all source branches belong to the measurement tree and all admittance branches to the cotree. In general, source branches are a subset of the twigs. Non-source twigs correspond to no network elements and do not represent a physical current path. Hence, t-s non-source twigs are introduced to complete a spanning tree. Note that the set of all sources can be the null set.

The measurement tree spans all network nodes twig terminal nodes define unique network node pairs. These node pairs can be considered ports. Hence, the cotree represents a multiport network.

It is desirable to obtain a set of equations which describe the steady state behavior of the multiport network in terms of its port variables. By assumption, the phasor equation describing any admittance branch k is given by

$$I_k = y_{k1} V_1 + y_{k2} V_2 + \ldots + y_{kk} V_k + \ldots + y_{k\hat{\ell}} V_{\hat{\ell}} \tag{2.1.5}$$

where,

$\hat{\ell}$ = number of admittance branches (links)

y_{kk} = self-admittance of link k

y_{ki} = mutual admittance between links k and i.

It follows from Eq. (2.1.5) that the phasor equations describing all admittance branches (primitive equations) are given in matrix form as

$$\underline{I}_\ell = Y_\ell \, \underline{V}_\ell \tag{2.1.6}$$

where

$Y_\ell = \hat{\ell} \times \hat{\ell}$ primitive admittance matrix.

From Eqs. (2.1.1) and (2.1.2) it can be shown that

$$-\underline{I}_t = Q_\ell \, \underline{I}_\ell \tag{2.1.8}$$

$$\underline{V}_\ell = -B_t \, \underline{V}_t \tag{2.1.9}$$

Thus, the negative of the port currents are a linear combination of link currents. Link voltages are a linear combination of port voltages.

From Eq. (2.1.3) it can be shown that

$$-B_t = Q_\ell^T \, . \tag{2.1.10}$$

It follows that Eq. (2.1.9) can be rewritten as

$$\underline{V}_\ell = Q_\ell^T \, \underline{V}_t \tag{2.1.11}$$

Premultiplying Eq. (2.1.6) by the cotree partition of the fundamental cutset matrix yields

$$Q_\ell \underline{I}_\ell = Q_\ell \, Y_\ell \, \underline{V} \tag{2.1.12}$$

Substituting Eqs. (2.1.8) and (2.1.11) into Eq. (2.1.12) gives

$$-\underline{I}_\ell = Q_\ell \, Y_\ell \, Q_\ell^T \, \underline{V}_t \tag{2.1.13}$$

Equation (2.1.13) describes the network steady state behavior in terms of port variables. For convenience, let the admittance matrix relating port currents to port voltages be given by

$$Y_t = Q_\ell \, Y_\ell \, Q_\ell^T \tag{2.1.14}$$

Thus, the network multiport equations are

$$\boxed{-\underline{I}_t = Y_t \, \underline{V}_t} \tag{2.1.15}$$

where Y_t is referred to as the multiport admittance matrix. Appendix A offers a development showing Y_{BUS} to be a special case of the multiport admittance matrix.

The set of all sources is known to be a subset of the twigs for a given measurement tree. If the set of all sources is not equal to the null set, then the multiport equations can be rewritten in terms of source-port variables only via a procedure known as "port suppression".[16]

Let Eq. (2.1.15) be reordered and partitioned such that

$$\begin{bmatrix} -\underline{I}_{t1} \\ \hline -\underline{I}_{t2} \end{bmatrix} = \left[\begin{array}{c|c} Y_{t11} & Y_{t12} \\ \hline Y_{t21} & Y_{t22} \end{array}\right] \begin{bmatrix} \underline{V}_{t1} \\ \\ \underline{V}_{t2} \end{bmatrix} \tag{2.1.16}$$

where

$\underline{I}_{t1}$ = s×1 vector of source-port currents

$\underline{I}_{t2}$ = h×1 vector of currents corresponding to ports without sources

$\underline{V}_{t1}$ = s×1 vector of source-port voltages

$\underline{V}_{t2}$ = h×1 vector of voltages corresponding to ports without sources

$\hat{t}$ = s+h, number of ports

If the terminal nodes of a non-source twig are incident to only branches belonging to the multiport network, then the non-source port current is zero. Thus, for the network of Fig. 2.1.1

$$\underline{I}_{t2} = \underline{0} \tag{2.1.17}$$

It follows that Eq. (2.1.17) can be separated into the two matrix equations

$$-\underline{I}_{t1} = Y_{t11}\,\underline{V}_{t1} + Y_{t12}\,\underline{V}_{t2} \tag{2.1.18}$$

$$\underline{0} = Y_{t21}\,\underline{V}_{t1} + Y_{t22}\,\underline{V}_{t2} \tag{2.1.19}$$

where,

Y_{t11} = s×s admittance matrix

Y_{t12} = s×h admittance matrix

Y_{t21} = h×s admittance matrix

Y_{t22} = h×h admittance matrix

Solving Eq. (2.1.19) for non-source port voltages yields

$$\underline{V}_{t2} = -Y_{t22}^{-1}\,Y_{t21}\,\underline{V}_{t1} \tag{2.1.20}$$

Substituting Eq. (2.1.20) into Eq. (2.1.18) gives

$$-\underline{I}_{t1} = (Y_{t11} - Y_{t12}\,Y_{t22}^{-1}\,Y_{t21})\underline{V}_{t1} \tag{2.1.21}$$

The multiport equations of Eq. (2.1.21) now describe the steady state behavior of the network in terms of source variables only. With non-source ports suppressed, the order of the multiport admittance matrix is s. In practical situations, s can be much less than $\hat{t}$.

Given the source voltages $\underline{V}_{t1}$, non-source port voltages and network link voltages can be recovered from Eqs. (2.1.20) and (2.1.11) respectively.

Simple Example

Consider the simple system shown in Fig. 2.1.2a. The admittance network (sources excluded) consists of six (6) admittance elements, each with a self admittance of 1.0℧. Two (2) of the elements are mutually coupled with a mutual admittance of 0.5℧.

Figure 2.1.2b shows the network graph with a measurement tree, defining ports, introduced. Darkened branches indicate twigs. Primitive equations describing the steady state behavior of the admittance network are given by

$$\begin{bmatrix} I_{\ell 1} \\ I_{\ell 2} \\ I_{\ell 3} \\ I_{\ell 4} \\ I_{\ell 5} \\ I_{\ell 6} \end{bmatrix} = \begin{bmatrix} 1.0 & -0.5 & 0 & 0 & 0 & 0 \\ -0.5 & 1.0 & 0 & 0 & 0 & 0 \\ 0 & 0 & 1.0 & 0 & 0 & 0 \\ 0 & 0 & 0 & 1.0 & 0 & 0 \\ 0 & 0 & 0 & 0 & 1.0 & 0 \\ 0 & 0 & 0 & 0 & 0 & 1.0 \end{bmatrix} \begin{bmatrix} V_{\ell 1} \\ V_{\ell 2} \\ V_{\ell 3} \\ V_{\ell 4} \\ V_{\ell 5} \\ V_{\ell 6} \end{bmatrix} \qquad (2.1.22)$$

The fundamental cutset matrix corresponding to the specified measurement tree is given by

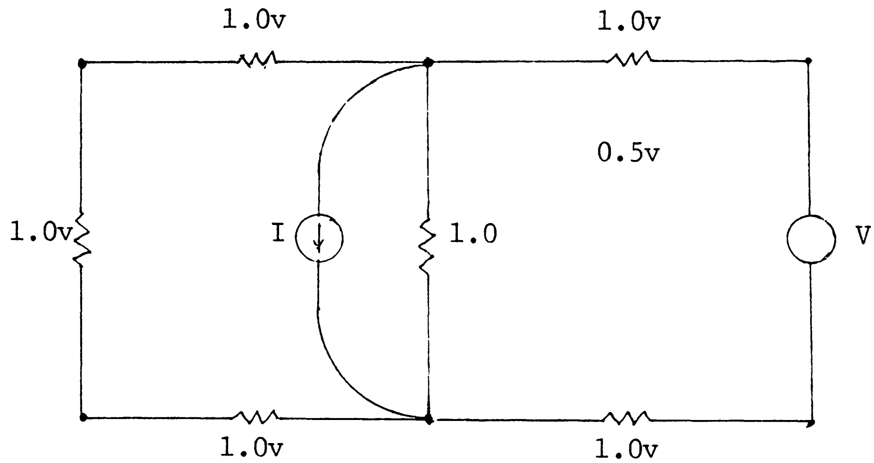

Fig. 2.1.2a. Simple network.

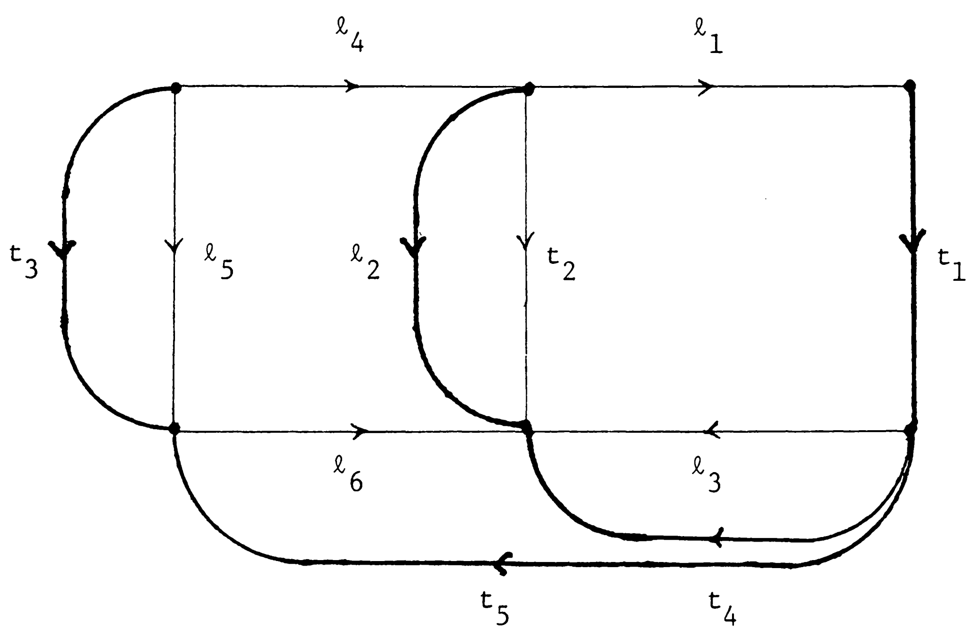

Fig. 2.1.2b. Network graph with measurement tree.

$$
\begin{array}{c} \\ t_1 \\ t_2 \\ Q = t_3 \\ t_4 \\ t_5 \end{array}
\begin{array}{c}
\begin{array}{ccccc:cccccc} t_1 & t_2 & t_3 & t_4 & t_5 & \ell_1 & \ell_2 & \ell_3 & \ell_4 & \ell_5 & \ell_6 \end{array} \\
\left[\begin{array}{ccccc:cccccc}
1 & 0 & 0 & 0 & 0 & -1 & 0 & 0 & 0 & 0 & 0 \\
0 & 1 & 0 & 0 & 0 & 1 & 1 & 0 & -1 & 0 & 0 \\
0 & 0 & 1 & 0 & 0 & 0 & 0 & 0 & 1 & 1 & 0 \\
0 & 0 & 0 & 1 & 0 & -1 & 0 & 1 & 1 & 0 & 1 \\
0 & 0 & 0 & 0 & 1 & 0 & 0 & 0 & -1 & 0 & -1
\end{array}\right]
\end{array}
\qquad (2.1.23)
$$

The network multiport admittance matrix, Y_t, is now given by

$$
Y_t = Q_\ell \, Y_\ell \, Q_\ell^T = \begin{bmatrix}
1.0 & -0.5 & 0 & 1.0 & 0 \\
-0.5 & 2.0 & -1.0 & -1.5 & 1.0 \\
0 & -1.0 & 2.0 & 1.0 & -1.0 \\
1.0 & -1.5 & 1.0 & 4.0 & -2.0 \\
0 & 1.0 & -1.0 & -2.0 & 2.0
\end{bmatrix} \qquad (2.1.24)
$$

Thus, the network steady state behavior expressed in terms of port variables is given by

$$
-\left[\begin{array}{c} I_{t_1} \\ I_{t_2} \\ \hline I_{t_3} \\ I_{t_4} \\ I_{t_5} \end{array}\right]
=
\left[\begin{array}{cc|ccc}
1.0 & -0.5 & 0 & 1.0 & 0 \\
-0.5 & 2.0 & -1.0 & -1.5 & 1.0 \\
\hline
0 & -1.0 & 2.0 & 1.0 & -1.0 \\
1.0 & -1.5 & 1.0 & 4.0 & -2.0 \\
0 & 0 & 1.0 & -2.0 & 2.0
\end{array}\right]
\left[\begin{array}{c} V_{t_1} \\ V_{t_2} \\ \hline V_{t_3} \\ V_{t_4} \\ V_{t_5} \end{array}\right] \qquad (2.1.25)
$$

Equation (2.1.25) is partitioned so as to indicate source ports and non-source ports.

The steady state behavior of the network can be described in terms of source port variables only. From Eq. (2.1.21) it follows that

$$-\begin{bmatrix} I_{t_1} \\ I_{t_2} \end{bmatrix} = \left[\begin{bmatrix} 1.0 & -0.5 \\ -0.5 & 2.0 \end{bmatrix} - \begin{bmatrix} 0 & 1.0 & 0 \\ -1.0 & -1.5 & 1.0 \end{bmatrix} \begin{bmatrix} 2.0 & 1.0 & -1.0 \\ 1.0 & 4.0 & -2.0 \\ -1.0 & -2.0 & 2.0 \end{bmatrix}^{-1} \begin{bmatrix} 0 & -1.0 \\ 1.0 & -1.5 \\ 0 & 1.0 \end{bmatrix}\right] \begin{bmatrix} V_{t_1} \\ V_{t_2} \end{bmatrix} \tag{2.1.26}$$

Thus, the network multiport equations, after port suppression, are given by

$$-\begin{bmatrix} I_{t_1} \\ I_{t_2} \end{bmatrix} = \begin{bmatrix} 0.500 & -0.250 \\ -0.250 & 1.208 \end{bmatrix} \begin{bmatrix} V_{t_1} \\ V_{t_2} \end{bmatrix} \tag{2.1.27}$$

2.2 General Methodology Applied to Power System Segments

Application of the general methodology to the multiport modeling of power system segments requires that the power system be represented as a directed graph. To this end, power systems will be defined as sources and loads connected by an admittance network. All system loads are specified as constant complex power sources.

The admittance network connecting sources and loads consists of admittance elements modeling power system components which can be inductively and/or capacitively coupled.

When the admittance network is represented as a directed graph, a segment is defined as follows:

> A set of connected and/or mutually coupled branches. All segments must include at least one branch. Each network branches belong to one and only one segment.

The admittance network of a power system consists of three principal segment types: (1) conductor segments, (2) transformer segments, and (3) auxiliary device segments. Multiport equations for the three segment types will be developed.

Conductor Segments

Consider the conductor segment shown in Fig. 2.2.1. Here, n-1 conductors are positioned above and parallel to the earth's surface. The earth's surface is considered a homogeneous medium of nonzero resistivity.

A number of techniques for developing lumped parameter models of parallel conductors with earth return exist.[17,18] For the purposes of this development, Carson's equations are employed.[19] Much literature has been devoted to Carson's equations.[20,21] Hence, only the applicable results are considered.

Carson's equations allow for inductive coupling between all segment conductors where the earth's surface is modeled as an equivalent conductor. Carson's results indicate that the steady state behavior of the segment is given by

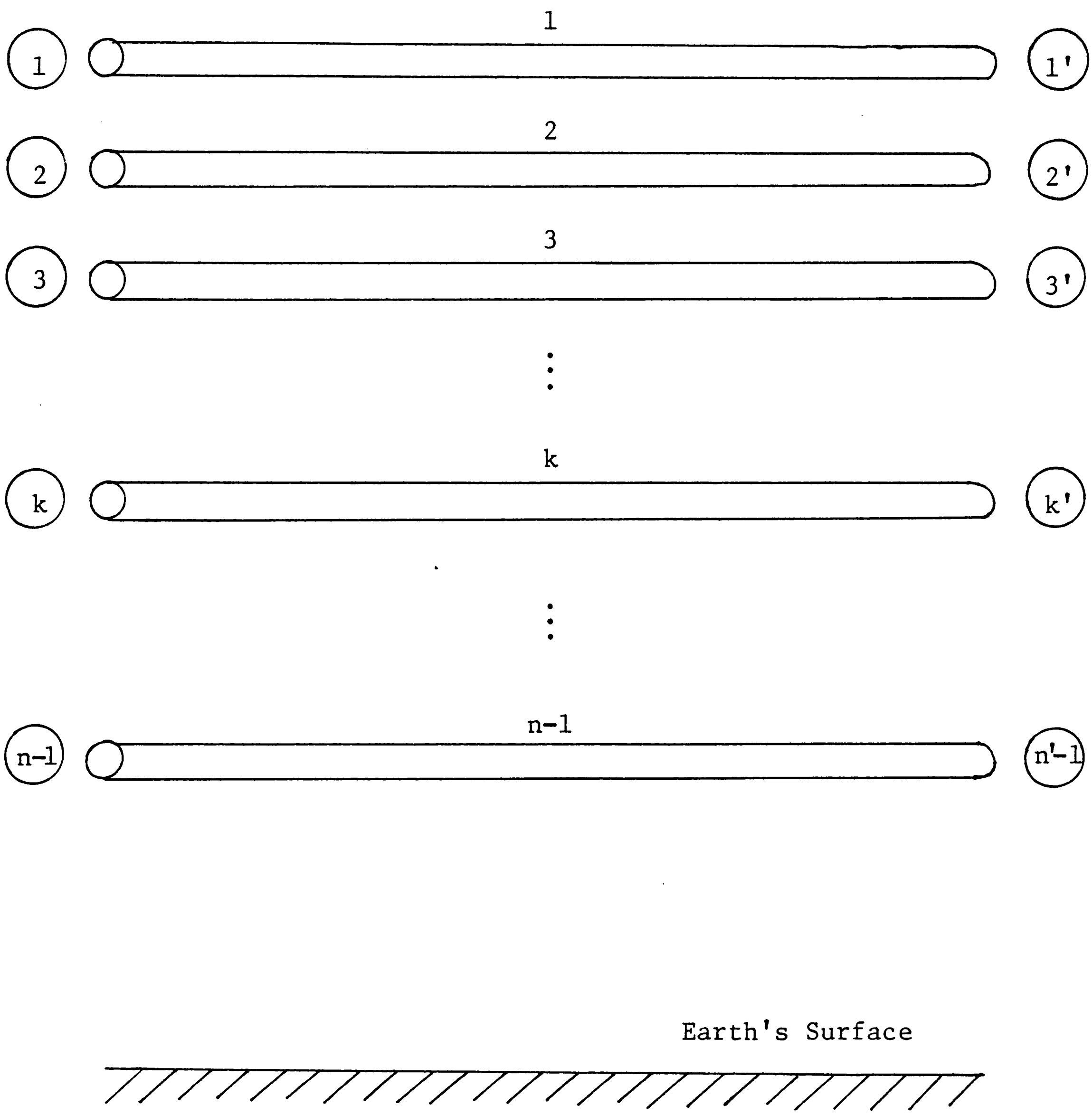

Fig. 2.2.1. Conductor segment of n-1 conductors above and parallel to the earth's surface.

$$\underline{V}_{P_L} = Z_{P_L} \underline{I}_{P_L} \tag{2.2.1}$$

where,

$\underline{V}_{P_L}$ = n×1 vector of voltages across conductors

$\underline{I}_{P_L}$ = n×1 vector of currents through conductors

Z_{P_L} = n×n impedance matrix (on-diagonal elements are self impedances, off diagonal elements are mutual reactances).

The directed graph corresponding to the conductor segment inductive effects and Eq. (2.2.1) is shown in Fig. 2.2.2.

Each conductor segment includes a single earth equivalent (ground) conductor. A segment of n conductors has 2n nodes, n nodes at each end of the segment. The terminal nodes of the ground conductor are referred to as ground nodes. Terminal nodes of neutral conductors are neutral nodes and terminal nodes of phase conductors are phase nodes.

Equation (2.2.1) is often formulated in a manner such that the conductor currents $\underline{I}_{P_L}$ sum to zero.[20] This added constraint suggests that current through the ground conductor is a linear combination of all other segment conductor currents. When this constraint is enforced, the ground conductor of Fig. 2.2.1 must be suppressed. With the ground conductor suppressed, the ground conductor branch of Fig. 2.2.2 is eliminated while its terminal nodes (ground nodes) remain a part of the segment graph.

The n nodes at a given end of a segment are said to "correspond", indicating that they are terminal nodes at the <u>same</u> end of the segment. Thus, a ground node can have no more than n-1 corresponding phase nodes. Similarly, a neutral node can have no more than n-2

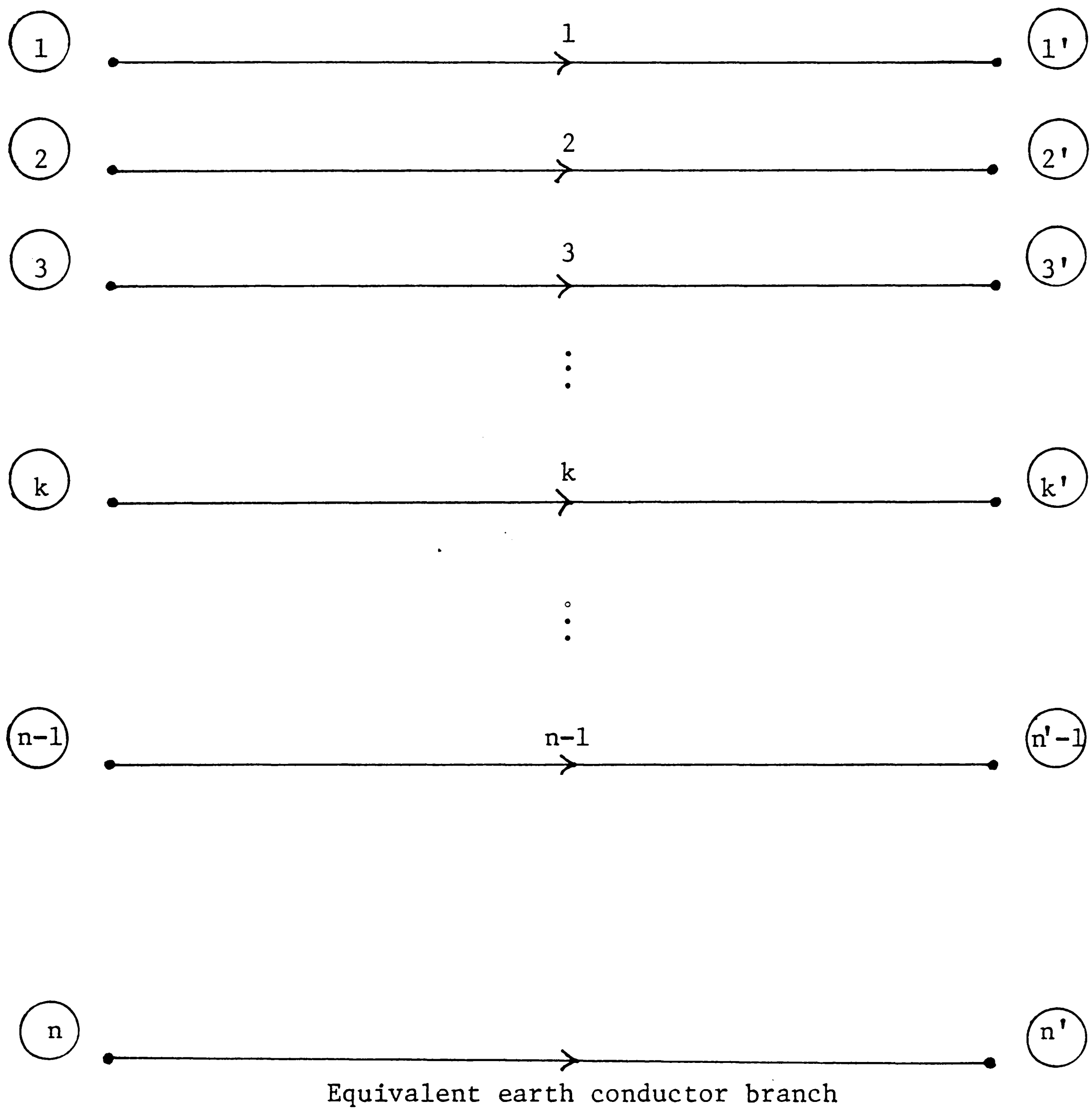

Fig. 2.2.2. Directed graph of conductor segment inductive effects.

corresponding phase nodes.

In addition to inductive coupling effects, long conductor segments can exhibit capacitive coupling between conductors. Modeling of capacitive coupling most often relies on the method of images.[22] Much literature has been devoted to the modeling of power conductor capacitive coupling by the method of images.[20,21,23] Only the applicable results are considered here. Although not exact, experience has shown this method is a realistic approximation.

At the relatively low frequencies characteristic of power systems, conductors are assumed to have linear charge density. The earth's surface is considered a perfectly conducting ground plane. Under these assumptions, it is possible to express voltages between conductors and the earth's surface as a function of conductor charge by

$$V = P\underline{q} \tag{2.2.2}$$

where,

$\underline{V}$ = $(n-1)\times 1$ conductor to earth voltage vector

$\underline{q}$ = $(n-1)\times 1$ charge vector

P = $(n-1)\times(n-1)$ potential matrix

The potential matrix P is known to be nonsingular; thus, Eq. (2.2.2) can be rewritten as

$$\underline{q} = P^{-1}\,\underline{V} \tag{2.2.3}$$

The elements of P^{-1} are called Maxwell's coefficients.[23,24]

The capacitive coupling between any two conductors and between any conductor and the earth can be determined from Eq. (2.2.3). The coupling can be represented by lumped capacitors as is shown in Fig. 2.2.3. The lumped capacitors model distributed capacitance across the length of the segment.

The effects of capacitive coupling are reasonably approximated by splitting lumped capacitors and connecting them between corresponding nodes at either end of the conductor segment. Thus, each capacitor incident to k^{th} conductor of Fig. 2.2.3 is split into two capacitors which sum to the original. Split capacitors are placed between the terminal nodes of appropriate conductors as shown in Fig. 2.2.4a.

In the phasor domain, the capacitors of Fig. 2.2.4a are admittance network elements. The directed graph representing the capacitive coupling of conductor k is shown in Fig. 2.2.4b. For an n conductor segment, the number of branches "d" needed to represent capacitive coupling effects of all segment conductors is given by

$$d = \frac{n!}{(n-2)!} \qquad (2.2.4)$$

The primitive equations describing conductor segment branches that represent capacitive coupling are given by

$$\underline{I}_{p_c} = Y_{p_c} \underline{V}_{p_c} \qquad (2.2.5)$$

where,

$\underline{I}_{p_c}$ = d×1 vector of currents through capacitive branches

$\underline{V}_{p_c}$ = d×1 vector of voltages across capacitances branches

Y_{p_c} = d×d vector diagonal admittance matrix.

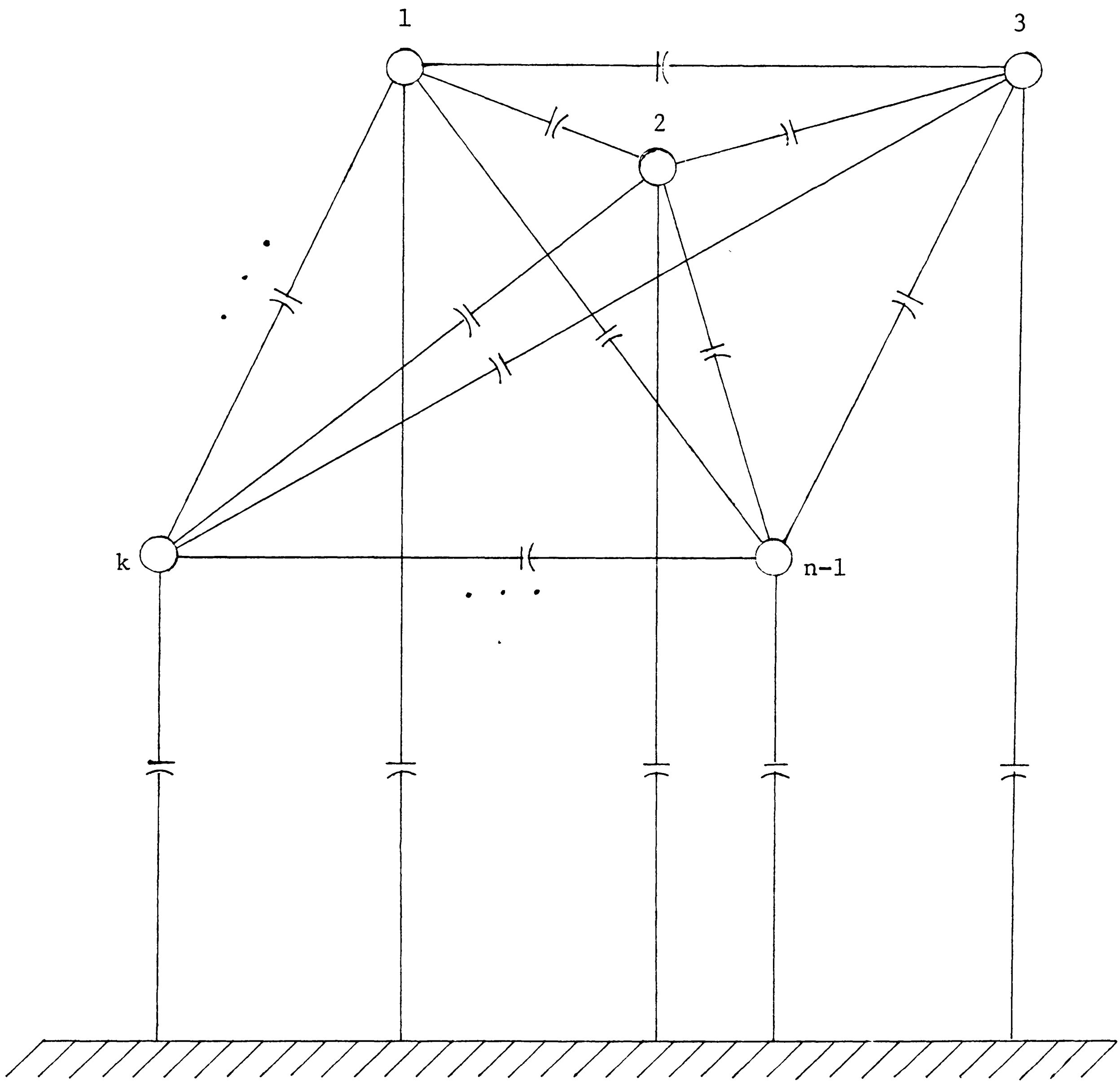

Fig. 2.2.3. Lumped capacitance between conductors and earth.

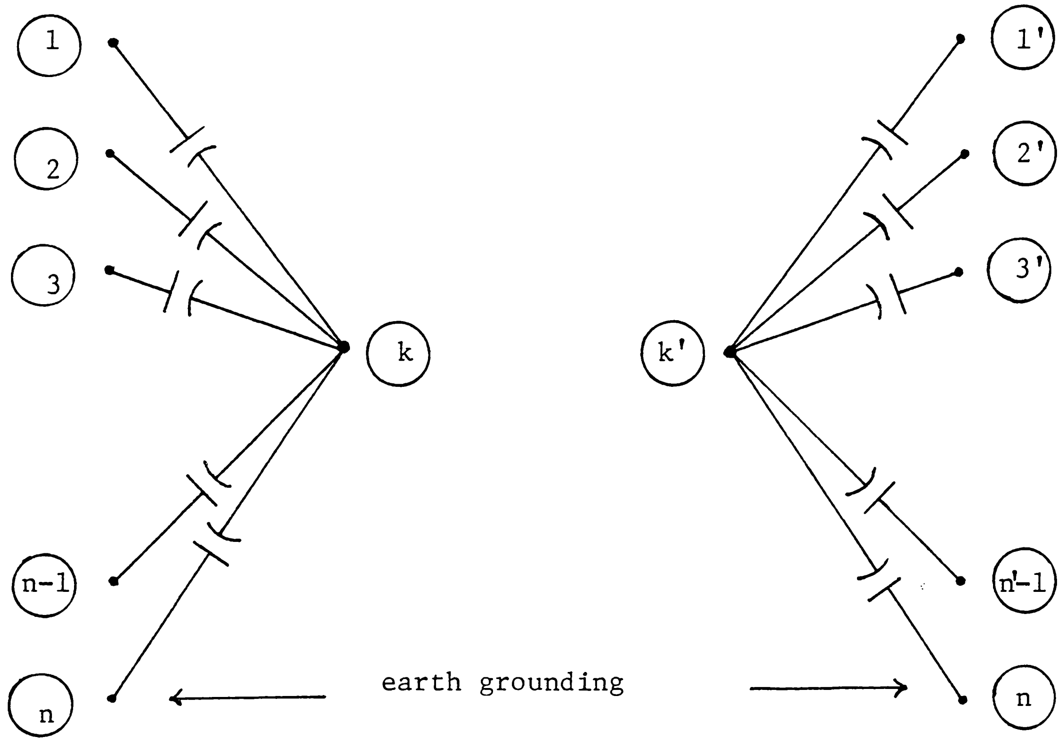

Fig. 2.2.4a. Lumped capacitance of k^{th} conductor split between corresponding segment nodes.

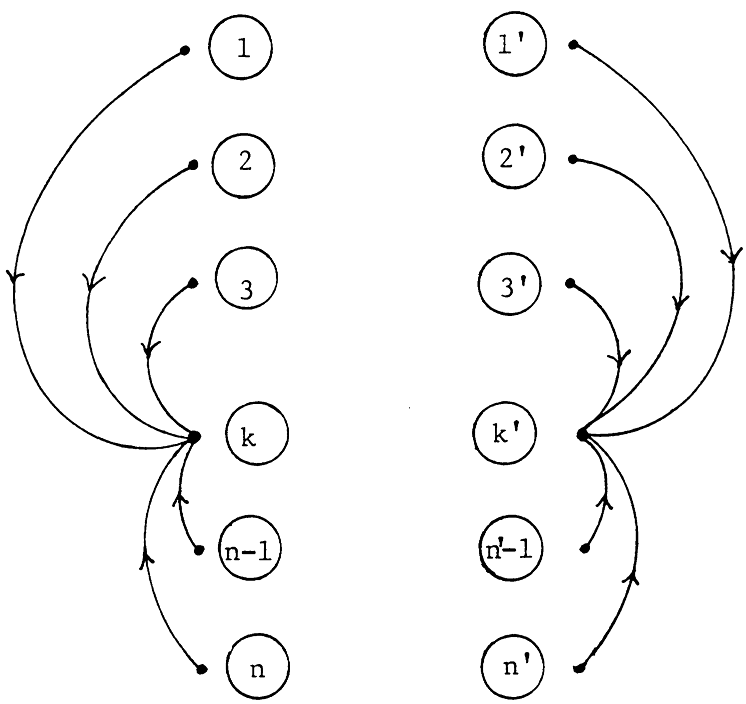

Fig. 2.2.4b. Direct graph representing capacitive coupling of the k^{th} conductor.

The complete graph of the conductor segment is given by the union of graphs representing inductive effects and capacitive effects. A graph representing the segment of Fig. 2.2.1 is shown in Fig. 2.2.5. (For convenience, only capacitive branches corresponding to the k^{th} conductor are shown.)

The steady state behavior of the conductor segment is given by

$$\underline{I}_p = Y_p \underline{V}_p \tag{2.2.6}$$

where,

$\underline{I}_p = [\underline{I}_{P_L}^T \ \underline{I}_{P_C}^T]^T$, (n+d)×1 vector of branch currents

$\underline{V}_p = [\underline{V}_{P_L}^T \ \underline{V}_{P_C}^T]^T$, (n+d)×1 vector of branch voltages

$Y_p = \left[\begin{array}{c|c} Z_{P_L}^{-1} & 0 \\ \hline 0 & Y_{P_C} \end{array}\right]$, (n+d)×(n+d) admittance matrix.

Equation (2.2.6) describes a general segment of overhead conductors. It is recognized that the segment can include any number of multiphase lines. If neutral phases are present, each neutral will have a set of corresponding power phases. It is noted that equations describing segments of underground cable can be obtained[25] and an analogous graph constructed.

The conductor segment of Fig. 2.2.1 can be considered a multiport network. The general methodology is to be applied such that port variables are in a suitable voltage reference frame for state estimation.

It follows that a measurement tree must include twigs defining ports in the phase-voltage reference frame. Thus, the following rule

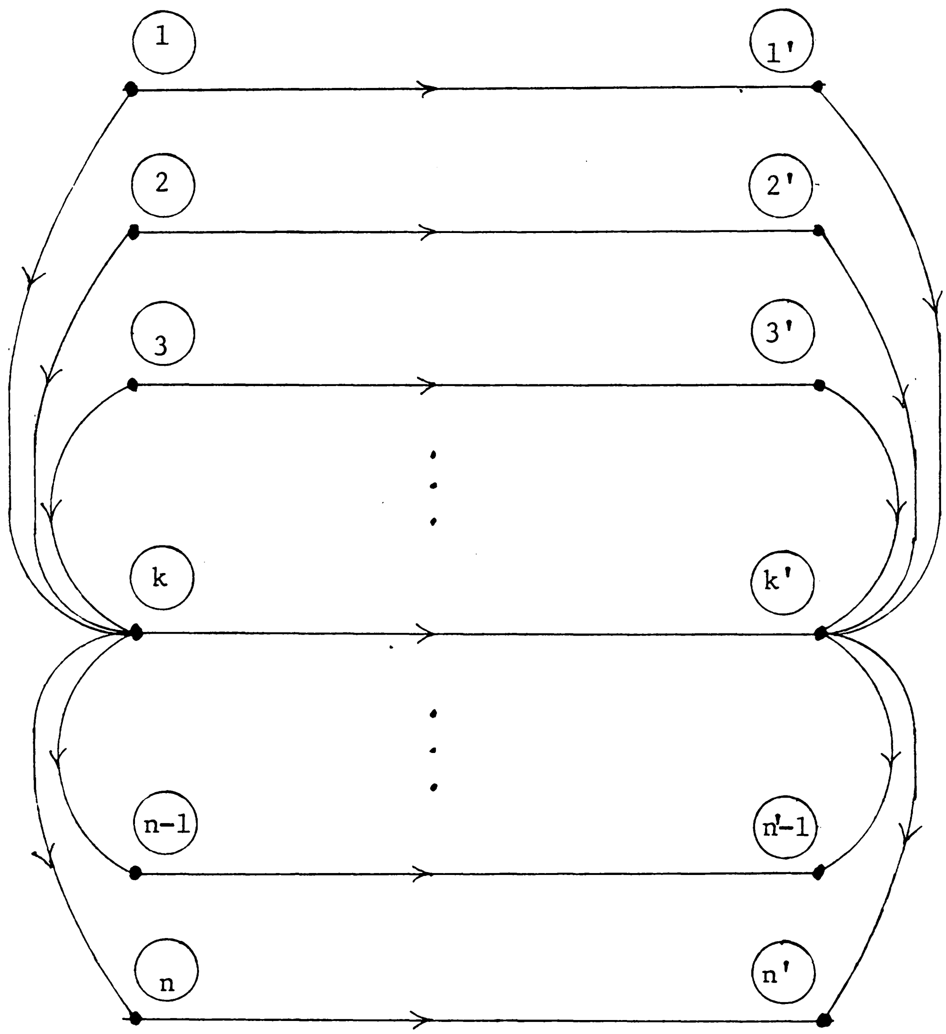

Fig. 2.2.5. Graph of conductor segment.

for introducing conductor segment measurement trees is given.

> A twig is introduced between ground nodes. Twigs are introduced between ground nodes and their corresponding neutral nodes. Twigs are introduced between neutral nodes and all of their corresponding phase nodes. If no neutral conductor is present, twigs are introduced between ground nodes and all of their corresponding phase nodes. Ground and neutral nodes can be coincident.

If the 1^{st} conductor is neutral, the measurement tree for the conductor segment of Fig. 2.2.1 is shown in Fig. 2.2.6. With the introduction of a measurement tree, the graph of Fig. 2.2.5 becomes the segment cotree.

Let the segment port voltages and port currents be written as

$\underline{V}_m$ = (2n-1) vector of segment port voltages

$\underline{I}_m$ = (2n-1) vector of segment port currents.

From Eqs. (2.1.8) and (2.1.11) it is known that

$$-\underline{I}_m = Q_p \, \underline{I}_p \tag{2.2.7}$$

$$\underline{V}_p = Q_p^T \, \underline{V}_m \tag{2.2.8}$$

where,

Q_p = cotree partition of the fundamental cutset matrix corresponding to the given measurement tree.

Premultiplying Eq. (2.2.6) by Q_p and substituting Eqs. (2.2.7) and (2.2.8) yields

$$-\underline{I}_m = Q_p \, Y_p \, Q_p^T \, \underline{V}_m \tag{2.2.9}$$

Equation (2.2.9) give the segment multiport equations and are rewritten as

$$-\underline{I}_m = Y_m \, \underline{V}_m \tag{2.2.10}$$

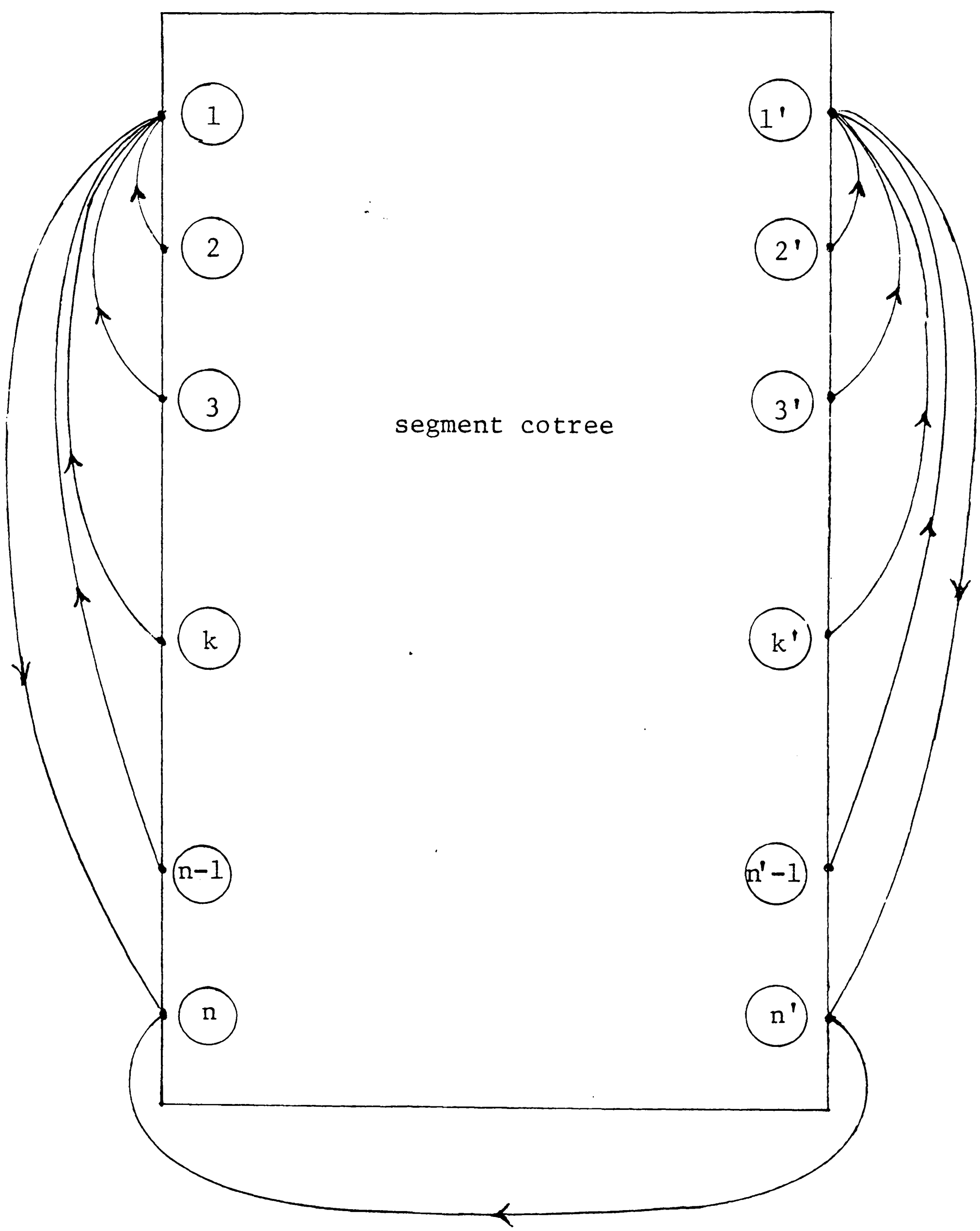

Fig. 2.2.6. Segment measurement tree impressed on the cotree.

where

$Y_m = Q_p\ Y_p\ Q_p^T$, the segment multiport admittance matrix.

Complex power flow in the phase conductors can be determined from the segment multiport equations. Let complex power flowing in the k^{th} conductor be denoted as $T_{kk'} + jU_{kk'}$ indicating the flow from node k to node k' as would be measured at node k.

Clearly, the complex power injected into the k^{th} conductor at node k is the negative of the k^{th} port complex power. Thus complex conductor flow is given by

$$T_{kk'} + jU_{kk'} = V_{m_k}\ I_{m_k}^* \tag{2.2.11}$$

where,

V_{m_k} = voltage across phase port k

I_{m_k} = current through phase port k.

Equation (2.2.11) can be rewritten in terms of multiport admittance matrix elements and port voltages

$$T_{kk'} + jU_{kk'} = V_{m_k} \sum_{i=1}^{2n-1} Y_{m_{ki}}^*\ V_{m_i}^* \tag{2.2.12}$$

where

$Y_{m_{ki}}$ = element of the multiport admittance matrix in the row corresponding to port k and the i^{th} column.

Hence, line flows can be given as a function of port variables only.

Equation (2.2.10) suggests that the segment can be graphically represented by the measurement tree alone. That is, the conductor segment is represented as the set of mutually coupled branches shown in Fig. 2.2.7. This graph is called the modified segment. Primitive equations describing the modified segment are given by

$$\underline{I}_m = Y_m \underline{V}_m \qquad (2.2.13)$$

Transformer Segments

Consider the circuit of Fig. 2.2.8a representing a nonideal two-winding transformer. Winding losses are reflected to the primary side; core losses are not considered.

Transformer banks are often modeled as a set of two-winding transformers appropriately interconnected. Here, multiport transformer segment models will consider only segments with two-winding transformers. Multiports for segments of three-winding and tap-changing transformers are given in Appendices B and C respectively.

The transformer of Fig. 2.2.8a is described by the following two port equations

$$-\begin{bmatrix} I_1 \\ I_2 \end{bmatrix} = \begin{bmatrix} y_t & -ay_t \\ -ay_t & a^2 y_t \end{bmatrix} \begin{bmatrix} V_1 \\ V_2 \end{bmatrix} \qquad (2.2.14)$$

where,

y_t = transformer loss admittance

a = reciprocal of the turns ratio.

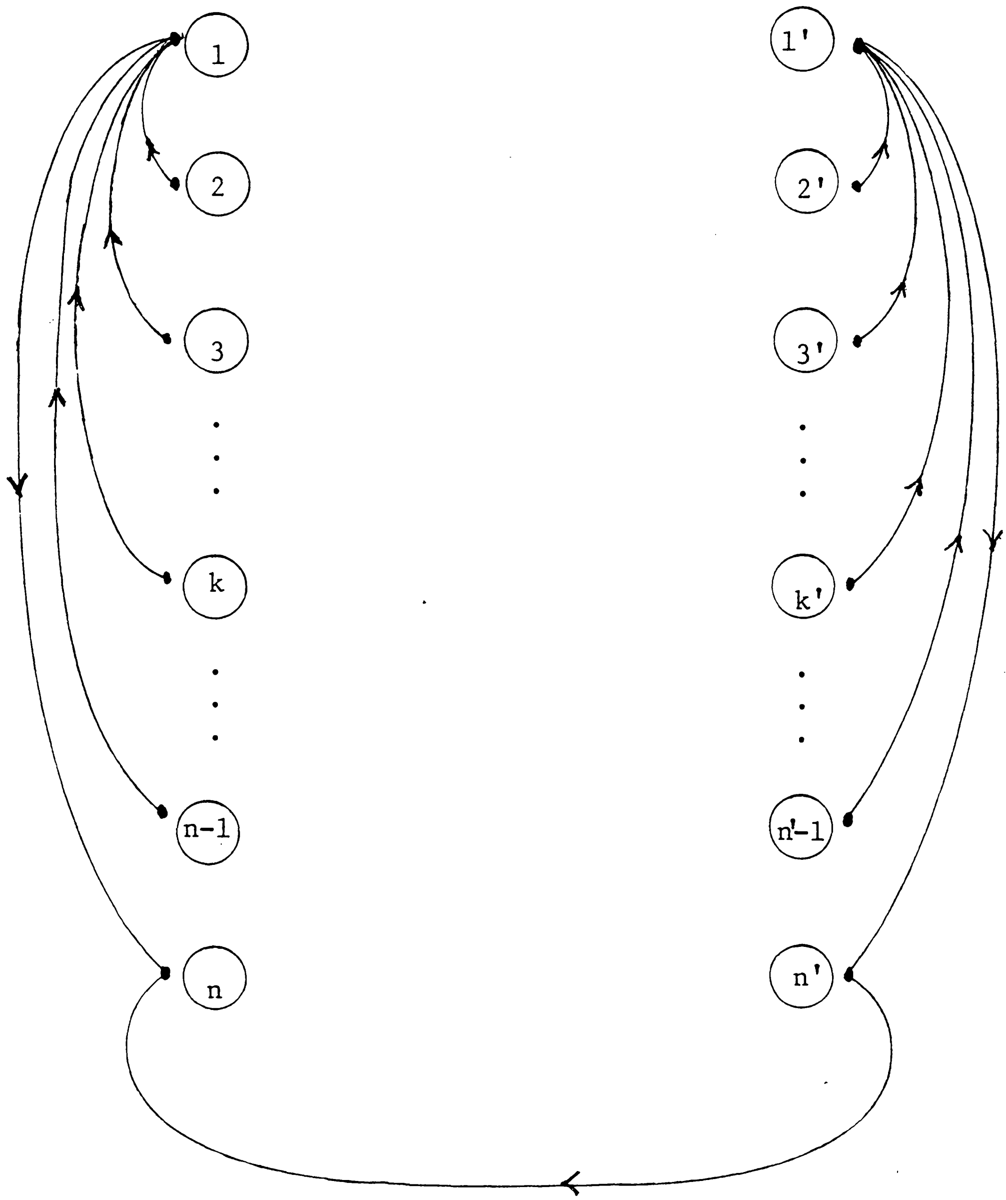

Fig. 2.2.7. Modified segment primitive.

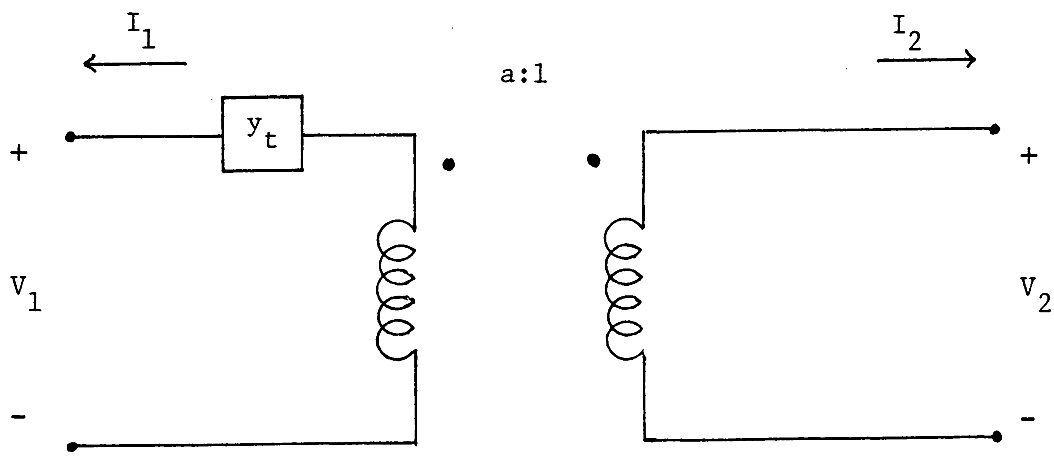

Fig. 2.2.8a. Two winding transformer.

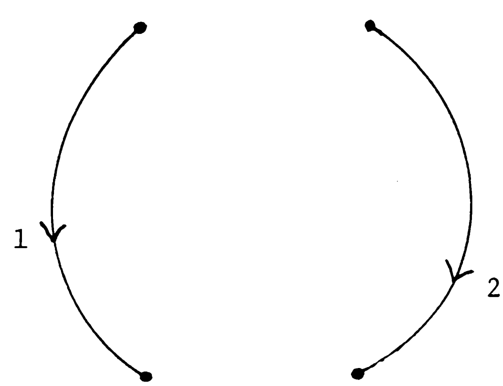

Fig. 2.2.8b. Transformer primitive branches.

Equation (2.2.14) suggest that the transformer can be represented by the two mutually coupled branches shown in Fig. 2.2.8b. These branches are called transformer primitive branches. The primitive equations for these branches are given by

$$-\begin{bmatrix} I_1 \\ I_2 \end{bmatrix} = \begin{bmatrix} y_t & -ay_t \\ -ay_t & a^2 y_t \end{bmatrix} \begin{bmatrix} V_1 \\ V_2 \end{bmatrix} \tag{2.2.15}$$

With transformers represented by primitive branches, transformer segments are defined as follows:

A set of connected transformer primitive branches and admittance branches. Admittance branches represent grounding admittances. The segment has only one ground node.

Primitive equations for a transformer segment are given by

$$\begin{bmatrix} \underline{I}_{p_T} \\ \hline \underline{I}_{p_g} \end{bmatrix} = \left[\begin{array}{c|c} Y_{p_T} & 0 \\ \hline 0 & Y_{p_g} \end{array}\right] \begin{bmatrix} \underline{V}_{p_T} \\ \underline{V}_{p_g} \end{bmatrix} \tag{2.2.16}$$

where,

$\underline{I}_{p_T}$ = vector of currents through transformer primitive branches

$\underline{I}_{p_g}$ = vector of currents through grounding admittance branches

$\underline{V}_{p_T}$ = vector of voltages across transformer primitive branches

$\underline{V}_{p_g}$ = vector of voltages across grounding admittance branches

Y_{p_T} = block diagonal matrix of transformer admittances

Y_{p_g} = diagonal admittance matrix.

For convenience, let Eq. (2.2.16) be rewritten as

$$\underline{I}_p = Y_p \underline{V}_p \qquad (2.2.17)$$

Transformer segments can be considered multiports; hence, it is necessary to introduce a measurement tree such that defined ports are in the phase voltage reference frame.

Terminal nodes of transformer primitive branches define segment primary and secondary nodes (as with any transformer bank). Phase nodes of the primary correspond; phase nodes of the secondary correspond. If a neutral node (nodes) is present, it (they) can correspond to: (1) primary nodes only, (2) secondary nodes only, (3) both primary and secondary nodes. Neutral nodes can be coincident with the ground node (i.e. solidly grounded neutrals).

The transformer segment measurement tree is defined as follows:

> Twigs are introduced between the ground node and all neutral nodes not coincident with the ground. Twigs are introduced between all neutral nodes and their corresponding phase nodes. For phase nodes with no corresponding neutral, twigs are introduced between phase and ground.

The segment graph for a delta-wye (secondary grounded through an admittance) transformer bank is shown in Fig. 2.2.9a. The segment measurement tree is shown in Fig. 2.2.9b.

Transformer primitive and grounding admittance branches now comprise the segment cotree. With a segment measurement tree introduced, it is desirable to obtain multiport equations describing the steady state behavior of the segment in terms of port variables.

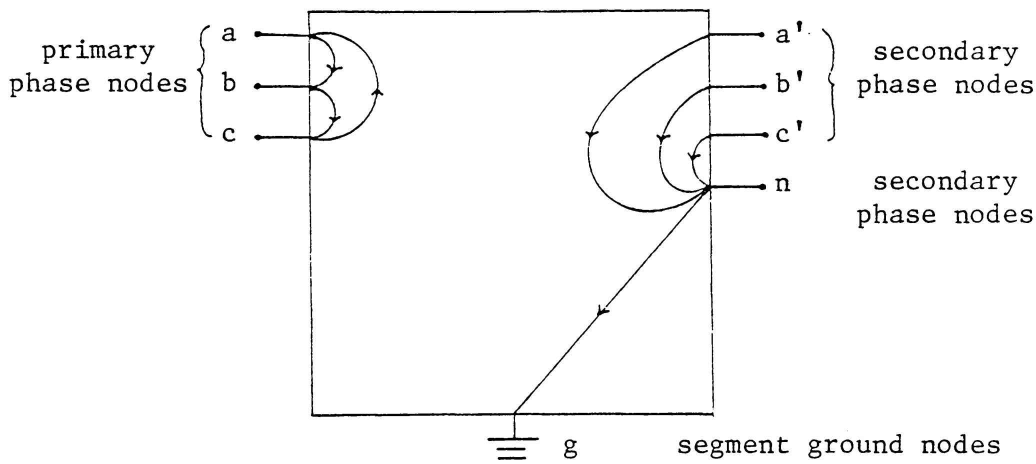

Fig. 2.2.9a. Delta-wye transformer bank segment with secondary grounding admittance.

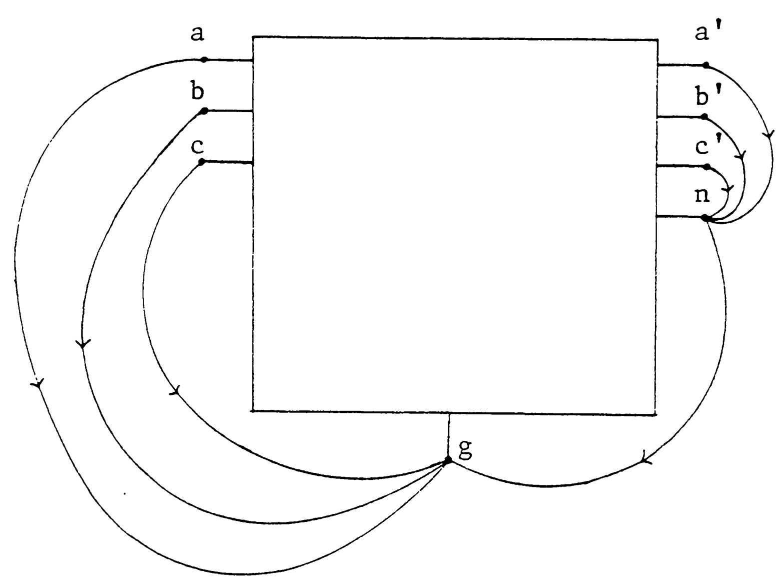

Fig. 2.2.9b. Delta-wye transformer bank segment with measurement tree.

For an n node transformer segment, let the segment port voltages, currents, and fundamental cutset matrix cotree partition be written as

$\underline{V}_m$ = $(n-1)\times 1$ vector of segment port voltages

$\underline{I}_m$ = $(n-1)\times 1$ vector of segment port currents

Q_p = cotree partition of the fundamental cutset matrix corresponding to a given segment measurement tree.

The segment cotree is described by Eq. (2.2.17). When the general methodology is employed, the segment multiport equations are given by

$$-\underline{I}_m = Q_p \, Y_p \, Q_p^T \, \underline{V}_m \tag{2.2.18}$$

For convenience, the segment multiport equations can be rewritten as

$$-\underline{I}_m = Y_m \, \underline{V}_m \tag{2.2.19}$$

where

$Y_m = Q_p \, Y_p \, Q_p^T$, $(n-1)\times(n-1)$ segment multiport admittance matrix.

Equation (2.2.19) suggests that the transformer segment can be graphically represented by its measurement tree alone. Thus, the segment is comprised of n-1 mutually coupled branches. These branches are called the modified primitive branches and collectively are called the modified segment. Equations describing the steady state behavior of the modified segment are given by

$$\underline{I}_m = Y_m \, \underline{V}_m \tag{2.2.20}$$

The modified segment for the delta-wye transformer bank of Fig. 2.2.9a is shown in Fig. 2.2.10.

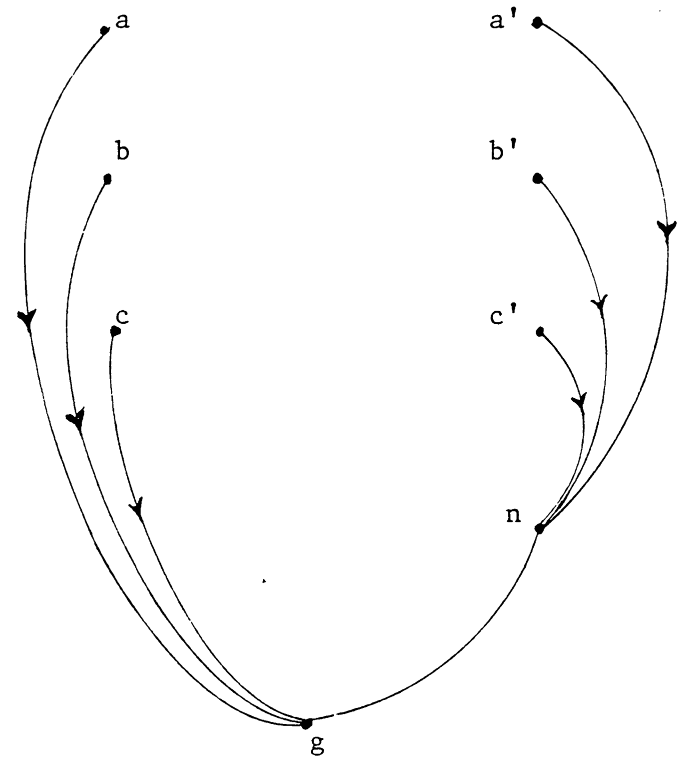

Fig. 2.2.10. Modified segment primitive for Delta-wye transformer bank.

Transformer segments, when modified, are described in the phase voltage reference frame and, thus, in terms of state variables.

Auxiliary Device Segments

Power systems often include auxiliary devices such as capacitor banks. It is assumed that any auxiliary device can be represented as a set of lumped admittances. When represented as a directed graph, auxiliary device segments are defined as follows:

> A set of connected admittance branches. Terminal nodes of the segment branches define phase nodes and no more than one neutral node. All segment nodes (phase and neutral) correspond to a single ground node. Ground and neutral nodes can be coincident.

The segment branches are assumed to be lumped admittances and the steady state behavior of the segment is given by

$$\underline{I}_p = Y_p \underline{V}_p \qquad (2.2.21)$$

where,

$\underline{I}_p$ = vector of segment branch currents

$\underline{V}_p$ = vector of segment branch voltages

Y_p = primitive admittance matrix.

Auxiliary device segments are considered multiport networks; thus, a segment measurement tree defining ports can be introduced. The segment measurement tree is defined as follows.

> A twig is introduced between the ground and neutral nodes. Twigs are introduced between all phase nodes and the neutral. If the ground and neutral are coincident or if no neutral is present, twigs are introduced between all phase nodes and ground.

With a segment measurement tree introduced, it is desirable to describe the segment steady state behavior in terms of port variables. The segment cotree is comprised of primitive admittance branches. Let the port voltages currents, and cotree partition of the fundamental cut-set matrix (corresponding to a specified measurement tree) be given by

$\underline{V}_m$ = vector of port voltages

$\underline{I}_m$ = vector of port currents

Q_p = cotree partition of the segment fundamental cutset matrix

When the general methodology is employed, multiport equations for the segment are given by

$$-\underline{I}_m = Q_p\, Y_p\, Q_p^T\, \underline{V}_m \tag{2.2.22}$$

A wye-connected capacitor bank with a grounding admittance is shown in Fig. 2.2.11a. The segment graph and measurement tree are shown in Fig. 2.2.11b.

Equation (2.2.22) suggests that an auxiliary device segment can be represented graphically by the segment measurement tree alone. Hence, the segment is represented as a set of mutually coupled branches called modified primitive branches. Collectively, the modified primitive branches are the modified segment. Equations describing the modified segment are given by

$$\underline{I}_m = Y_m\, \underline{V}_m \tag{2.2.23}$$

where,

$Y_m = Q_p\, Y_p\, Q_p^T$, segment multiport admittance matrix.

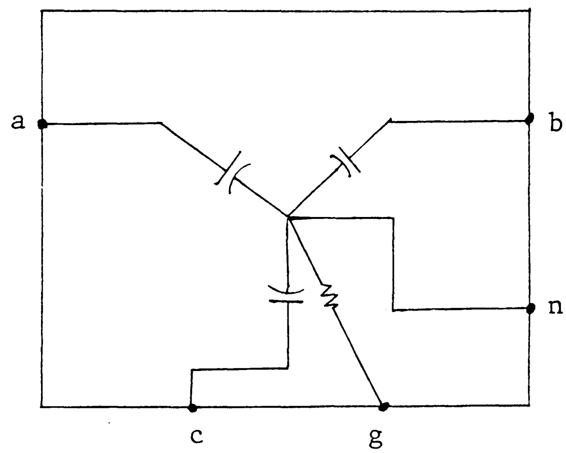

Fig. 2.2.11a. Wye-connected capacitor bank with grounding admittance.

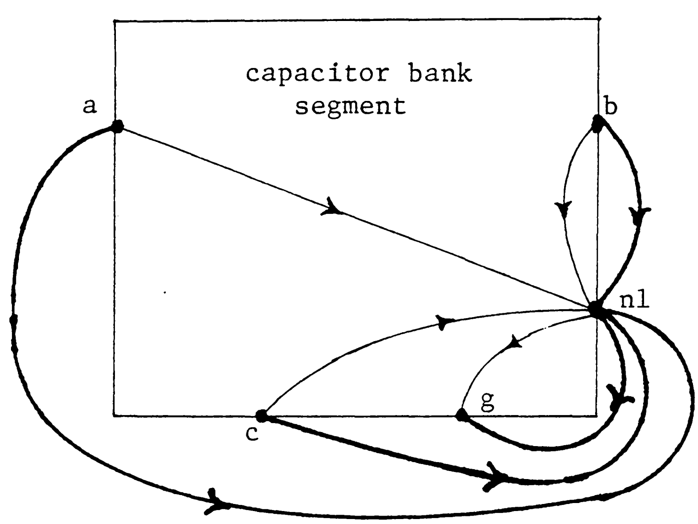

Fig. 2.2.11b. Capacitor bank segment graph and measurement tree.

The modified segment for the wye-connected capacitor bank of Fig. 2.2.11a is shown in Fig. 2.2.12.

2.3 General Methodology Applied to Power Systems

Having applied the general methodology to all power system segments, the power system admittance network (sources and loads excluded) is represented as the union of all modified segments. The union of all modified segments is called the <u>modified primitive network</u>. Equations describing the steady state behavior of the modified primitive network for a system of q segments is given by

$$\begin{bmatrix} \underline{I}_{m_1} \\ \underline{I}_{m_2} \\ \vdots \\ \underline{I}_{m_i} \\ \vdots \\ \underline{I}_{m_q} \end{bmatrix} = \begin{bmatrix} Y_{m_1} & 0 \ldots & 0 \ldots & 0 \\ 0 & Y_{m_2} \ldots & 0 \ldots & 0 \\ \vdots & \vdots \ddots & \vdots & \vdots \\ 0 & 0 \ldots & Y_{m_i} \ldots & 0 \\ \vdots & \vdots & \vdots \ddots & \vdots \\ 0 & 0 \ldots & 0 \ldots & Y_{m_q} \end{bmatrix} \begin{bmatrix} \underline{V}_{m_1} \\ \underline{V}_{m_2} \\ \vdots \\ \underline{V}_{m_i} \\ \vdots \\ \underline{V}_{m_q} \end{bmatrix} \qquad (2.3.1)$$

For convenience, Eq. (2.3.1) can be rewritten as

$$\underline{I}_m = Y_m \underline{V}_m \qquad (2.3.2)$$

where,

$\underline{I}_m$ = vector of modified primitive network currents

$\underline{V}_m$ = vector of modified primitive network voltages

Y_m = block diagonal admittance matrix. The diagonal blocks are segment multiport admittance matrices.

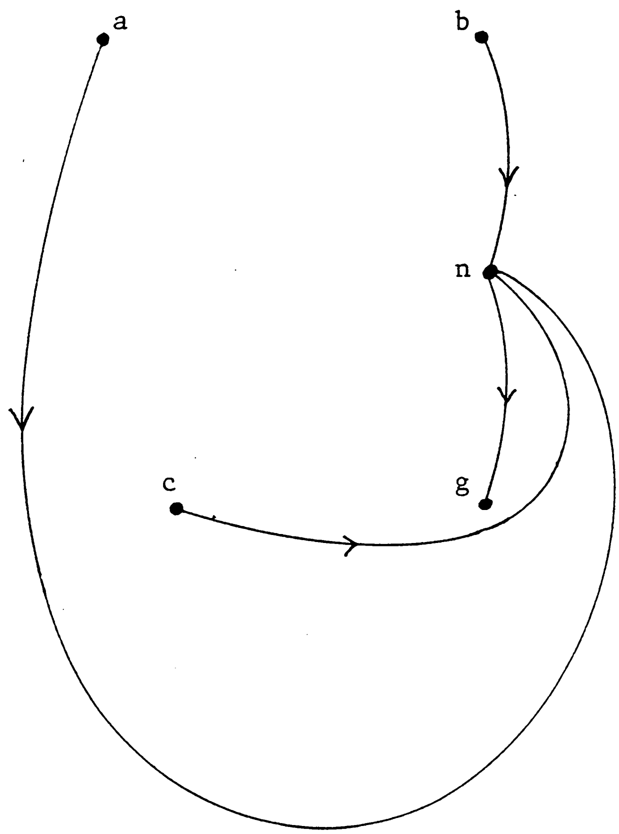

Fig. 2.2.12. Modified segment of wye-connected capacitor bank.

The modified primitive network can be considered a multiport network. It is desirable to describe the steady state behavior of the modified primitive network in terms of port variables. Hence, a network measurement tree defining system ports must be introduced.

The network measurement tree must define ports available to all system sources and loads. By assumption, all system unbalanced sources and loads are connected phase to neutral. All balanced delta connected sources and loads can be transformed into an equivalent wye connection. The modified primitive network is known to contain at least one and perhaps many ground nodes. One ground node is specified as the datum node.

The network measurement tree corresponding to the modified primitive network is defined as follows:

> Twigs are introduced between the datum node and all ground nodes. Twigs are introduced between all ground nodes (including the datum) and their corresponding neutral nodes. Twigs are introduced between all neutral nodes and their corresponding phase nodes. For phase nodes with no corresponding neutral, twigs are introduced between phase and ground. Ground nodes and neutral nodes can be coincident.

Consider the simple power system, shown in Fig. 2.3.1a, consisting of a delta-wye transformer bank segment, a 3-ϕ conductor segment with neutral, and a wye-connected capacitor bank (auxiliary device segment). The admittance network (system sources and loads excluded) is represented as the union of segment modified primitive branches as shown in Fig. 2.3.1b. The modified primitive network is considered a multiport network. Thus, a system measurement tree, defining system ports, is

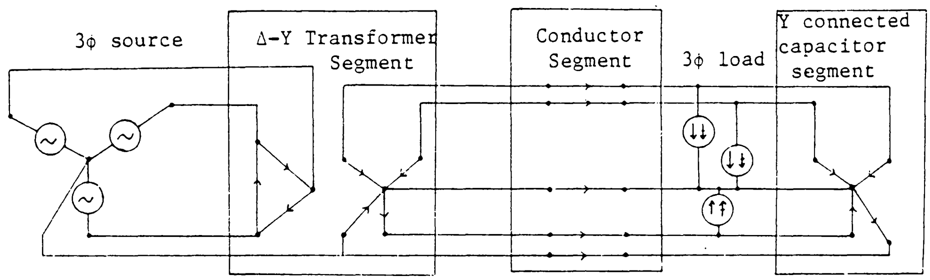

Fig. 2.3.1a. Simple power system.

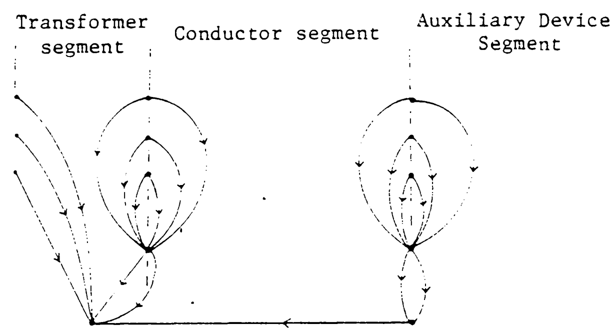

Fig. 2.3.1b. Modified primitive network (sources and loads excluded).

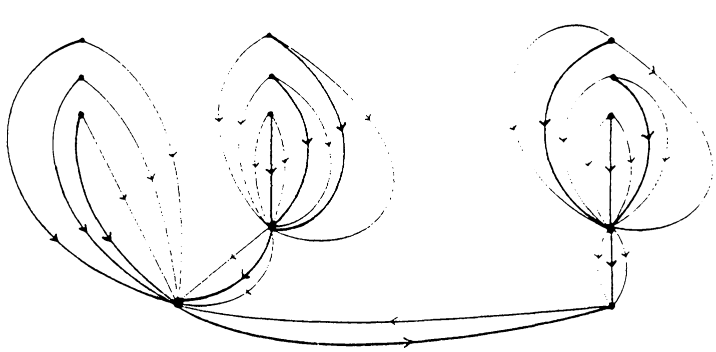

Fig. 2.3.1c. Modified primitive network with measurement tree.
Twigs are darkened branches.

introduced. The modified primitive network with the system measurement tree is shown in Fig. 2.3.1c.

With a system measurement tree introduced in the fashion described above, the following port definitions are offered: (1) a twig incident only to ground nodes defines a ground port, (2) a twig incident to neutral and ground nodes defines a neutral port, and (3) a twig incident to any phase node defines a phase port. State variables are phase port voltage magnitudes and angles. All system sources and loads are connected at available phase ports.

It follows that the general methodology can be used to obtain multiport equations for the modified primitive network. For a system of n nodes, let the system port voltages and currents be given by

$\underline{V}_t$ = (n-1) vector of system port voltages

$\underline{I}_t$ = (n-1) vector of system port currents.

By Eqs. (2.1.8) and (2.1.11) it can be shown that

$$-\underline{I}_t = Q_m \underline{I}_m \tag{2.3.3}$$

$$\underline{V}_m = Q_m^T \underline{V}_t \tag{2.3.4}$$

where,

Q_m = cotree partition of the fundamental cutset matrix corresponding to the system measurement tree and the modified primitive network.

Premultiplying Eq. (2.3.2) by the cotree partition of the cutset matrix yields

$$Q_m \underline{I}_m = Q_m Y_m \underline{V}_m \tag{2.3.5}$$

Substituting Eqs. (2.3.3) and (2.3.4) into Eq. (2.2.5) gives

$$-\underline{I}_t = Q_m \, Y_m \, Q_m^T \, \underline{V}_m \tag{2.3.6}$$

Equation (2.3.6) gives the power system multiport equations and can be rewritten as

$$-\underline{I}_t = Y_t \, \underline{V}_t \tag{2.3.7}$$

where,

$Y_t = Q_m \, Y_m \, Q_m^T$, (n-1)×(n-1) <u>system multiport admittance matrix</u>.

Hence, Eq. (2.3.6) describes the steady state behavior of a power system in terms of its port variables.

2.4 <u>Linear Dependence of Multiport Admittance Matrices and Normalization of Multiport Equations</u>

An important consideration with regard to multiport equations is linear dependence among equations. Linear dependence among equations obtained by the general methodology is reflected in the rank of the resulting multiport admittance matrix.

When the general methodology is applied to segments, the resulting segment multiport admittance matrices are often of non-zero nullity. Both segment topology and the nature of segment primitive equations can contribute to nullity.

<u>Topological Dependence</u>

Consider first, nullity resulting from segment topology. It can be shown that the number of independent multiport equations is related to the number of independent segment cutsets.[26] Thus, the rank of the multiport admittance matrix is less than or equal to the rank of the segment graph. Or,

$$r_{sm} \leq r_{sg} \tag{2.4.1}$$

where,

r_{sm} = rank of the segment multiport admittance matrix

r_{sg} = rank of the segment graph.

A component of a graph is defined as a connected subgraph containing the maximal number of branches.[26] It can be shown that for a segment of n nodes,

$$r_{sg} = n - c_{sg} \tag{2.4.2}$$

where,

c_{sg} = the number of segment graph components.

It follows that

$$r_{sm} \leq n - c_{sg} \,. \tag{2.4.3}$$

The nullity, h_{sm}, of a segment multiport admittance matrix is given by

$$h_{sm} = (n-1) - r_{sm} \tag{2.4.4}$$

From Eqs. (2.4.4) and (2.4.3) it can be shown that

$$h_{sm} \geq c_{sg} - 1 \tag{2.4.5}$$

Conductor segments can have negligible capacitive coupling effects. Graphs for such segments include more than one component. Thus, Eq. (2.4.5) can be used to establish nullity lower bounds for the resulting multiport admittance matrices.

Dependence of Primitive Equations

Linear dependence among primitive (modified primitive) equations can introduce nullity into multiport admittance matrices. When the general methodology is employed, the network multiport admittance matrix is given by Eq. (2.1.14), shown again here.

$$Y_t = Q_\ell \, Y_\ell \, Q_\ell^T \tag{2.4.6}$$

Let the following matrix ranks be given.

r_{y_t} = rank of the multiport admittance matrix Y_t

r_{y_ℓ} = rank of the primitive admittance matrix Y_ℓ

r_{Q_ℓ} = rank of the cutset matrix partition Q_ℓ

The rank r_{Q_ℓ} can be determined as in Eq. (2.4.2).

For a network of $\hat{t}$+1 nodes and $\hat{\ell}$ branches, linear dependence among the primitive equations implies that

$$r_{y_\ell} < \hat{\ell} \tag{2.4.7}$$

But from Sylvester's inequality, it is known that[27]

$$r_{y_t} \leq \min \, (r_{y_\ell}, \, r_{Q_\ell}).$$

Hence, for $r_{Q_\ell} < r_{y_\ell} < \hat{\ell}$, it is possible to lower bound the nullity of the multiport admittance matrix.

It is noted here that linear dependence among transformer primitive equations is found in Eq. (2.2.15). Thus, transformer segment multiport admittance matrices have nonzero nullity.

<u>Normalization of Multiport Equations</u>

Nominal phase voltage magnitudes can vary greatly throughout a given power system. For this reason, power system equations are most often normalized such that phase voltage magnitudes are nominally near unity.

A meaningful normalization scheme for unbalanced power systems requires that all state estimator equations be in per-unit. Hence, all segment primitive equations are normalized prior to application of the general methodology.

The following normalization scheme is used to obtain per-unit segment primitive equations.

1) A system power base, S_B (KVA), is selected. All system loads are normalized by S_B.
2) A base voltage V_{BC_i} (KV) is selected for the i^{th} conductor segment. Conductor segment base admittance is given by $Y_{BC_i} = S_B/V_{BC_i}^2$. Segment base current is given by $I_{BC_i} = S_B/V_{BC_i}$. All segment primitive admittances are normalized by Y_{BC_i}. All segment port voltages are normalized by V_{BC_i}. All segment port currents are normalized by I_{BC_i}.

3) A primary base voltage V_{BTP_i} (KV) and a secondary base voltage V_{BTS_i} (KV) is selected for the i^{th} transformer segment. The base turns ratio for segment transformers is given by $a_{BT_i} = V_{BTP_i}/V_{BTS_i}$. Segment primary base current is given by

$I_{BTP_i} = S_B/V_{BTP_i}$. Segment secondary base current is given by $I_{BTS_i} = S_B/V_{BTS_i}$. Transformer segment base admittance is given by $Y_{BT_i} = S_B/V^2_{BTP_i}$. All segment turns ratios are normalized by a_{BT_i}. All segment transformer loss admittances are normalized by Y_{BT_i}. All primary port voltages are normalized by V_{BTP_i}. All secondary port voltages are normalized by V_{BTS_i}. All primary port currents are normalized by I_{BTP_i}. All secondary port currents are normalized by I_{BTS_i}.

4) A base voltage V_{BA_i} (KV) is selected for the i^{th} auxiliary device segment. Segment base admittance is given by $Y_{BA_i} = S_B/V^2_{BA_i}$. Segment base current is given by $I_{BA_i} = S_B/V_{BA_i}$. All segment primitive admittances are normalized by Y_{BA_i}. All segment port voltages are normalized by V_{BA_i}. All segment port currents are normalized by I_{BA_i}.

5) All adjacent segment ports must have the same base voltage.

With all segment primitive equations normalized, the general methodology yields per-unit multiport equations. Segment port variables are de-normalized when multiplied by their corresponding base values.

By definition, system phase and neutral ports correspond directly to segment phase and neutral ports. Thus, system phase and neutral port variables are de-normalized when multiplied by corresponding segment port base values.

System ground ports are defined by twigs connected between the datum and ground nodes of the modified primitive network. Therefore, system ground ports, in general, can connect segments that are normalized on different base voltages. It follows that ground port base voltages are unknown. Note, however, that system ground port variables are of little practical interest. In the event that ground port voltages are needed, they can be recovered using real units. The ground voltages of practical are segment ground port voltages.

CHAPTER 3. STATE ESTIMATION OF UNBALANCED POWER SYSTEMS

State estimation of unbalanced power system, as developed in the sections that follow, appeals to the extended method of weighted least squares. Least squares estimators are widely accepted within the electric utility industry; hence, no attempt to examine the estimator's quality is made.

State estimator equations, to be developed, are a natural result of the multiport models offered in Chapter 2. Thus, the results offered in this chapter are intended to demonstrate that unbalanced power systems can be modeled such that accepted power system state estimation techniques can be employed.

The extended method of weighted least squares is developed in Sec. 3.1. The method is presented as a minimum norm estimator. No statistics are associated with the estimator or model.

Unbalanced power system estimator equations are formulated in Sec. 3.2. Rules for identifying state variables are given. Port suppression is employed to obtain multiport equations in terms of state voltages only. Equations for the estimator model are obtained from the suppressed multiport equations. Equations yielding entries of the Jacobian matrix are presented.

The extended method of weighted least squares of Sec. 3.1, along with the estimator equations of Sec. 3.2, are demonstrated by way of example in Sec. 3.3.

Example 1 seeks to demonstrate the estimator equations and modeling technique for a simple balanced power system. Inasmuch as balanced power systems represent a special case of unbalanced multiport networks, Example 1 verifies the estimator on a system with a well known solution.

Example 2 demonstrates the estimator equations and modeling technique for an unbalanced power system. Example 2 considers a system containing both load and topological imbalances.

3.1 Extended Method of Weighted Least Squares

Power system state estimation requires that a set of measured variables be functionally related to the system state. When the measured variables are noise corrupted, this relationship can be written as

$$\underline{z} = \underline{f}(\underline{x}) + \underline{\varepsilon} \qquad (3.1.1)$$

where,

$\underline{z}$ = m×1 vector of measured variables

$\underline{x}$ = n×1 state vector

$\underline{f}$ = m×1 nonlinear vector function

$\underline{\varepsilon}$ = m×1 error vector (noise)

$m < n$.

The extended method of weighted least squares defines the "best" estimate of the state, $\hat{\underline{x}}$, as that $\underline{x}$ which minimizes a weighted inner product of the error vector with itself. That is,

$$\min_{\underline{x}} J(\underline{x}) = \underline{\varepsilon}^T W \underline{\varepsilon} \qquad (3.1.2)$$

where,

$J(\underline{x})$ = scalar objective function

W = m×m symmetric positive definite weighting matrix

From Eq. (3.1.1), the objective function, Eq. (3.1.2), can be written as

$$\min_{\underline{x}} J(\underline{x}) = \left(\underline{z} - \underline{f}(\underline{x})\right)^T W\left(\underline{z} - f(\underline{x})\right) . \tag{3.1.3}$$

Consider first an approximation of the objective function

Expanding the vector function $\underline{f}$, via Taylor series, about an initial state $\underline{x}_o$ [28] it follows that

$$\underline{f}(\underline{x}) = \underline{f}(\underline{x}_o) + F(\underline{x}_o)(\underline{x} - \underline{x}_o) + \underline{g}(\underline{x}, \underline{x}_o) \tag{3.1.4}$$

where,

$$F(\underline{x}_o) = \left.\frac{\partial \underline{f}(\underline{x})}{\partial \underline{x}}\right|_{\underline{x} = \underline{x}_o} \text{, m×n Jacobian matrix evaluated at } \underline{x}_o$$

$\underline{g}(\underline{x}, \underline{x}_o)$ = vector of Taylor series higher order terms .

The vector function $\underline{f}$ is linearized about $\underline{x}_o$ by setting $\underline{g}$, the vector of higher order terms, to $\underline{o}$.

$$\tilde{\underline{f}}(\underline{x}) = \underline{f}(\underline{x}_o) + F(\underline{x}_o)(\underline{x} - \underline{x}_o) \tag{3.1.5}$$

Let the objective function, Eq. (3.1.3), be approximated by

$$\min_{\underline{x}} \tilde{J}(\underline{x}) = \left(\underline{z} - \underline{f}(\underline{x}_o) - F(\underline{x}_o)(\underline{x}-\underline{x}_o)\right)^T W\left(\underline{z} - \underline{f}(\underline{x}_o) - F(\underline{x}_o)(\underline{x}-\underline{x}_o)\right) \tag{3.1.6}$$

The value of $\underline{x}$ which minimizes $\tilde{J}(\underline{x})$ must satisfy the necessary conditions given by

$$\frac{\partial \tilde{J}(\underline{x})}{\partial \underline{x}} = \underline{0} \tag{3.1.7}$$

It follows from Eq. (3.1.6) that the necessary conditions can be written as

$$-2F^T(\underline{x}_o)\ W\left(\underline{z} - \underline{f}(\underline{x}_o)\right) + 2F^T(\underline{x}_o)\ WF(\underline{x}_o)(\underline{x} - \underline{x}_o) = 0 \tag{3.1.8}$$

Solving Eq. (3.1.8) for $\underline{x}$ gives the value $\tilde{\underline{x}}$ which minimizes the objective function $\tilde{J}(\underline{x})$. Hence, $\tilde{\underline{x}}$ is given by

$$\tilde{\underline{x}} = \underline{x}_o + \left(F^T(\underline{x}_o)\ WF(\underline{x}_o)\right)^{-1} F^T(\underline{x}_o)\ W\left(\underline{z} - \underline{f}(\underline{x}_o)\right) \tag{3.1.9}$$

Clearly, $\tilde{\underline{x}}$ exists only when the Jacobian matrix F is of full rank. When the Jacobian is of full rank the system is said to be <u>observable</u>.

The vector $\tilde{\underline{x}}$ closely approximates the best estimate $\hat{\underline{x}}$ only when the initial state $\underline{x}_o$ is sufficiently close to $\hat{\underline{x}}$. However, Eq. (3.1.9) can be extended to a Newton type iterative algorithm that converges to $\hat{\underline{x}}$. The iterative equation is given by

$$\tilde{\underline{x}}_{k+1} = \tilde{\underline{x}}_k + \left(F^T(\tilde{\underline{x}}_k)\ WF(\tilde{\underline{x}}_k)\right)^{-1} F^T(\tilde{\underline{x}}_k)\ W\left(\underline{z} - \underline{f}(\tilde{\underline{x}}_k)\right) \tag{3.1.10}$$

where,

k = iteration index.

When Eq. (3.1.10) is solved iteratively, iteration is continued until $\tilde{\underline{x}}_{k+1} \simeq \tilde{\underline{x}}_k$. That is,

$$|\tilde{\underline{x}}_{k+1} - \tilde{\underline{x}}_k| \le \underline{a} \tag{3.1.11}$$

where,

$\underline{a}$ = n×1 positive tolerance vector.

When Eq. (3.1.11) is satisfied, $\hat{\underline{x}} \simeq \tilde{\underline{x}}_k$.

Since the vector function $\underline{f}$ is nonlinear, $\tilde{\underline{x}}_k$ is, in general, a local minimum of $J(\underline{x})$. To insure that Eq. (3.1.10) converges to the true best estimate, an initial state sufficiently close to $\hat{\underline{x}}$ must be selected.

It can be shown that $\hat{\underline{x}}$ is "best linear unbiased" when the weighting matrix is selected such that[29]

$$W = \text{cov}^{-1}\ (\underline{\varepsilon}\ \underline{\varepsilon}^T)$$

where,

$\text{cov}(\underline{\varepsilon}\ \underline{\varepsilon}^T) = E(\underline{\varepsilon}\ \underline{\varepsilon}^T)$.

There can exist estimators with statistical properties superior to those of the extended method of least squares (ie. some nonlinear estimator). Other estimators are considered beyond the scope of this dissertation.

In applying the extended method of least squares to power system state estimation, the statistics of measurement noise are most often unknown. Thus, no statistical inference is drawn from the estimator. The weighting matrix W is specified heuristically.

3.2 Estimator Equations for Unbalanced Power Systems

The problem statement for power system state estimation, from Sec. 1.1, is taken as given. It is assumed that the set of measured variables $\underline{z}$ are selected such that the system is observable. Hereafter, all equations are assumed per-unit.

The segment and system multiport equations of Chapter 2 are used to obtain equations relating measured variables of $\underline{z}$ to the state $\underline{x}$. Thus, the vector function $\underline{f}$ can be formulated.

Let the vector of measured variables (measurement vector) be partitioned such that

$$\underline{z} = \begin{bmatrix} \underline{P} \\ \underline{Q} \\ \underline{T} \\ \underline{U} \\ \underline{E} \end{bmatrix} \tag{3.2.1}$$

where,

$\underline{P}$ = vector of measured load real powers

$\underline{Q}$ = vector of measured load reactive powers

$\underline{T}$ = vector of measured conductor real power flows

$\underline{U}$ = vector of measured conductor reactive power flows

$\underline{E}$ = vector of measured phase voltage magnitudes.

All measured variables are phase port variables. Real load powers, reactive load powers, and phase voltage magnitudes are system phase port variables. Conductor real and reactive power flows are segment phase port variables.

Let the state vector be partitioned such that

$$\underline{x} = \begin{bmatrix} \underline{\delta} \\ \underline{V} \end{bmatrix} \tag{3.2.2}$$

where,

$\underline{\delta}$ = vector of state voltage angles

$\underline{V}$ = vector of state voltage magnitudes.

The state voltages are a subset of the system phase port voltages.

Given the system and segment port variables belonging to $\underline{z}$, it is necessary to identify the system port voltages belonging to $\underline{x}$. By definition, system measurement twigs appear across all segment phase ports. Hence, each segment phase port is said to have a corresponding system phase port. Note that one system phase port can have many corresponding segment phase ports.

Three subsets of system phase ports can be identified.

1) The L subset, defined as the set of ports across which sources or loads are connected.
2) The E subset, defined as the set of ports at which phase voltage magnitudes are measured.
3) The F subset, defined as the set of system ports which correspond to segment ports at which conductor power flows are measured.

The state voltages are identified as follows.

The voltage across any port belonging to subsets L, E, or F is taken as a state voltage.

Having identified the state voltages, system and segment multiport equations can be formulated in terms of only state voltages.

System Multiport Equations

Consider the system multiport equations given by

$$-\underline{I}_t = Y_t \, \underline{V}_t \qquad (3.2.3)$$

Let Eq. (3.2.3) be reordered and partitioned such that

$$-\begin{bmatrix} \underline{I}_{t_R} \\ \underline{I}_{t_N} \end{bmatrix} = \begin{bmatrix} Y_{t_{RR}} & Y_{t_{RN}} \\ Y_{t_{NR}} & Y_{t_{NN}} \end{bmatrix} \begin{bmatrix} \underline{V}_{t_R} \\ \underline{V}_{t_N} \end{bmatrix} \qquad (3.2.3)$$

where,

$\underline{I}_{t_R}$ = vector of currents through ports belonging to L, E, or F

$\underline{I}_{t_N}$ = vector of currents through ports not belonging to L, E, or F

$\underline{V}_{t_R}$ = vector of state voltages

$\underline{V}_{t_N}$ = vector of voltages across ports not belonging to L, E, or F

Given that all system sources and loads are connected at ports belonging to L, any system port not in L has zero current. It follows that

$$\underline{I}_{t_N} = \underline{0} \; . \qquad (3.2.5)$$

Equations (3.2.4) and (3.2.5) suggest that port suppression can be employed to obtain the desired multiport equations. Separating Eq. (3.2.4) into two equations yields

$$-\underline{I}_{t_R} = Y_{t_{RR}} \underline{V}_{t_R} + Y_{t_{RN}} \underline{V}_{t_N} \tag{3.2.6}$$

$$\underline{0} = Y_{t_{NR}} \underline{V}_{t_R} + Y_{t_{NN}} \underline{V}_{t_N} \tag{3.2.7}$$

Solving Eq. (3.2.7) for $\underline{V}_{t_N}$ gives

$$\underline{V}_{t_N} = -Y_{t_{NN}}^{-1} Y_{t_{NR}} \underline{V}_{t_R} \tag{3.2.8}$$

Substituting Eq. (3.2.8) into Eq. (3.2.6) yields

$$-\underline{I}_{t_R} = (Y_{t_{RR}} - Y_{t_{RN}} Y_{t_{NN}}^{-1}) \underline{V}_{t_R} \tag{3.2.9}$$

Equation (3.2.9) gives the system multiport equations in terms of only state voltages. For convenience, Eq. (3.2.9) is written as

$$-\underline{I}_{t_R} = Y_{t_R} \underline{V}_{t_R} \tag{3.2.10}$$

where,

$Y_{t_R} = (Y_{t_{RR}} - Y_{t_{RN}} Y_{t_{NN}}^{-1} Y_{t_{NR}})$, suppressed system multiport admittance matrix.

<u>Segment Multiport Equations</u>

The segment multiport equations can be formulated in terms of only state voltages. Consider the set of all segment multiport equations, for a system of q segments, given by the matrix equation

$$
-\begin{bmatrix} \underline{I}_{m_1} \\ \underline{I}_{m_2} \\ \vdots \\ \underline{I}_{m_i} \\ \vdots \\ \underline{I}_{m_q} \end{bmatrix} = \begin{bmatrix} Y_{m_1} & 0 \ldots 0 \ldots 0 \\ 0 & Y_{m_2} \ldots 0 \ldots 0 \\ \vdots & \vdots \ddots \vdots \quad \vdots \\ 0 & 0 \ldots Y_{m_i} \ldots 0 \\ \vdots & \vdots \quad \vdots \ddots \vdots \\ 0 & 0 \ldots 0 \ldots Y_{m_q} \end{bmatrix} \begin{bmatrix} \underline{V}_{m_1} \\ \underline{V}_{m_2} \\ \vdots \\ \underline{V}_{m_i} \\ \vdots \\ \underline{V}_{m_q} \end{bmatrix} \tag{3.2.11}
$$

Equation (3.2.11) is more concisely written as

$$
-\underline{I}_m = Y_m \underline{V}_m \tag{3.2.12}
$$

From Eq. (2.3.3), segment port voltages are a linear combination of system port voltages. Equation (2.3.3) is given again here;

$$
\underline{V}_m = Q_m^T \underline{V}_t \tag{3.2.13}
$$

where,

Q_m = the cotree partition of the fundamental cutset matrix for a given system measurement tree and modified primitive network.

Substituting Eq. (3.2.13) into Eq. (3.2.12) yields

$$
-\underline{I}_m = Y_M \underline{V}_t \tag{3.2.14}
$$

where,

$Y_M = Y_m Q_m^T$, nonsquare admittance matrix relating segment port currents to system port voltages.

Equation (3.2.14) can be reordered and partitioned such that

$$-\underline{I}_m = \left[Y_{M_R} \;\middle|\; Y_{M_N} \right] \begin{bmatrix} \underline{V}_{t_R} \\ \hline \underline{V}_{t_N} \end{bmatrix} \tag{3.2.15}$$

Recognizing from Eq. (3.2.8) that $\underline{V}_{t_N}$ can be given in terms of state voltages, Eq. (3.2.14) is written as

$$-\underline{I}_m = \left[Y_{M_R} \;\middle|\; Y_{M_N} \right] \begin{bmatrix} U_R \\ \hline -Y_{t_{NN}}^{-1} \; Y_{t_{NR}} \end{bmatrix} \underline{V}_{t_R} \tag{3.2.16}$$

where,

U_R = identity matrix, dimensions compatable with $\underline{V}_{t_R}$.

Equation (3.2.16) is given more concisely as

$$-\underline{I}_m = Y_{m_R} \, \underline{V}_{t_R} \tag{3.2.17}$$

where,

$$Y_{m_R} = \left[Y_{M_R} \;\middle|\; Y_{M_N} \right] \begin{bmatrix} U_R \\ \hline -Y_{t_{NN}}^{-1} \; Y_{t_{NR}} \end{bmatrix},$$

nonsquare admittance matrix relating segment port currents to state voltages.

Estimator Model

The complex power S at any phase port (system or segment) can be formulated. The nonlinear vector function $\underline{f}$ (estimator model) is, in part, determined from complex port powers.

Given Eq. (3.2.10), the complex power S_{t_i} (= P_i + j Q_i) of the i^{th} system phase port is written as

$$S_{t_i} = -V_i \, e^{j\delta_i} \sum_{j=1}^{g} y_{t_{ij}} \, e^{-j\Theta_{t_{ij}}} \, V_j \, e^{-j\delta_j} \qquad (3.2.18)$$

where,

$V_i \, e^{j\delta_i}$ = i^{th} entry of $\underline{V}_{t_R}$ (state voltages)

$y_{t_{ij}} \, e^{j\Theta_{t_{ij}}}$ = $(i,j)^{th}$ entry of Y_{t_R}

g = number of state voltages .

Given Eq. (3.2.17), the complex power S_{m_i} (= T_i + j U_i) of the i^{th} segment phase port is written as

$$S_{m_i} = -V_{m_i} \, e^{j\delta_{m_i}} \sum_{j=1}^{g} y_{m_{ij}} \, e^{-j\Theta_{m_{ij}}} \, V_j \, e^{-j\delta_j} \qquad (3.2.19)$$

where,

$V_{m_i} \, e^{j\delta_{m_i}}$ = voltage across the i^{th} segment phase port

$y_{m_{ij}} \, e^{j\Theta_{m_{ij}}}$ = $(i,j)^{th}$ entry of Y_{m_R} .

However, the voltage across the i^{th} segment phase port is known to equal the voltage across its corresponding system phase port. Let the k^{th} system phase port correspond to the i^{th} segment phase port. When the k^{th} system port belongs to subset F, Eq. (3.2.19) can be rewritten as

$$S_{m_i} = -V_k e^{j\delta_k} \sum_{j=1}^{g} y_{m_{ij}} e^{-j\Theta_{m_{ij}}} V_j e^{-j\delta_j} \qquad (3.2.20)$$

Equations (3.2.18) and (3.2.20) are used to express elements of the measurement subvectors $\underline{P}$, $\underline{Q}$, $\underline{T}$, and $\underline{U}$ as nonlinear functions of the state variables.

Let the ℓ^{th} load real power measurement P_ℓ be taken from the i^{th} system phase port. It follows from Eq. (3.2.18) that

$$P_\ell = -\sum_{j=1}^{g} V_i y_{t_{ij}} V_j \cos(\delta_i - \Theta_{t_{ij}} - \delta_j) + \varepsilon_{P_\ell} \qquad (3.2.21)$$

Let the ℓ^{th} load reactive power measurement Q_ℓ be taken from the i^{th} system phase port. It follows from Eq. (3.2.18) that

$$Q_\ell = -\sum_{j=1}^{g} V_i y_{t_{ij}} V_j \sin(\delta_i - \Theta_{t_{ij}} - \delta_j) + \varepsilon_{Q_\ell} \qquad (3.2.22)$$

Let the ℓ^{th} conductor real power flow measurement T_ℓ be taken from the i^{th} segment phase port. It follows from Eq. (3.2.20) that

$$T_\ell = -\sum_{j=1}^{g} V_k y_{m_{ij}} V_j \cos(\delta_k - \Theta_{m_{ij}} - \delta_j) + \varepsilon_{T_\ell} \qquad (3.2.23)$$

Let the ℓ^{th} conductor reactive power flow measurement U_ℓ be taken from the i^{th} segment phase port. It follows from Eq. (3.2.20) that

$$U_\ell = -\sum_{j=1}^{g} V_k y_{m_{ij}} V_j \sin(\delta_k - \Theta_{m_{ij}} - \delta_j) + \varepsilon_{U_\ell} \qquad (3.2.24)$$

The phase voltage magnitude measurements are easily formulated in terms of the state variables. Let the ℓ^{th} phase voltage magnitude measurement E_ℓ be taken from the i^{th} system phase port. It follows that

$$E_\ell = V_i + \varepsilon_{E_\ell} \ . \tag{3.2.25}$$

Entries of the nonlinear vector function are taken from Eqs. (3.2.21) - (3.2.25), thus, formulating the deterministic estimator model. The iterative algorithm given by Eq. (3.1.10) given by Eq. (3.1.10) requires the Jacobian matrix F. Equations formulating the entries of F are obtained from Eqs. (3.2.21) - (3.2.25).

The Jacobian, when partitioned so as to be compatable with Eqs. (3.2.1) and (3.2.2), is given by

$$F = \left[\begin{array}{c|c} \dfrac{\partial \underline{P}}{\partial \underline{\delta}} & \dfrac{\partial \underline{P}}{\partial \underline{V}} \\ \hline \dfrac{\partial \underline{Q}}{\partial \underline{\delta}} & \dfrac{\partial \underline{Q}}{\partial \underline{V}} \\ \hline \dfrac{\partial \underline{T}}{\partial \underline{\delta}} & \dfrac{\partial \underline{T}}{\partial \underline{V}} \\ \hline \dfrac{\partial \underline{U}}{\partial \underline{\delta}} & \dfrac{\partial \underline{U}}{\partial \underline{V}} \\ \hline \dfrac{\partial \underline{E}}{\partial \underline{\delta}} & \dfrac{\partial \underline{E}}{\partial \underline{V}} \end{array}\right] \tag{3.2.26}$$

Let the ℓ^{th} measurement in each subvector P, Q, T, and U correspond to the i^{th} system (segment) phase port. The following twenty (20) equations give the Jacobian matrix entries as partial derivatives with respect to state variables of Eqs. (3.2.21) - (3.2.25).

$$\frac{\partial P_\ell}{\partial \delta_i} = \sum_{\substack{j=1\\ j\neq i}}^{q} V_i\, y_{t_{ij}}\, V_j \sin(\delta_i - \Theta_{t_{ij}} - \delta_j) \tag{3.2.27}$$

$$\frac{\partial P_\ell}{\partial \delta_j} = -\, V_i\, y_{t_{ij}}\, V_j \sin(\delta_i - \Theta_{t_{ij}} - \delta_j) \tag{3.2.28}$$

$$\frac{\partial P_\ell}{\partial V_i} = -2V_i\, y_{t_{ii}} \cos(-\Theta_{t_{ii}}) - \sum_{\substack{j=1\\ j\neq 1}}^{g} y_{y_{ij}}\, V_j \cos(\delta_i - \Theta_{t_{ij}} - \delta_j) \tag{3.2.29}$$

$$\frac{\partial P_\ell}{\partial V_j} = -V_i\, y_{t_{ij}} \cos(\delta_i - \Theta_{t_{ij}} - \delta_j) \tag{3.2.30}$$

$$\frac{\partial Q_\ell}{\partial \delta_i} = -\sum_{\substack{j=1\\ j\neq 1}}^{g} V_i\, y_{t_{ij}}\, V_j \cos(\delta_i - \Theta_{t_{ij}} - \delta_j) \tag{3.2.31}$$

$$\frac{\partial Q_\ell}{\partial \delta_j} = V_i\, y_{t_{ij}}\, V_j \cos(\delta_i - \Theta_{t_{ij}} - \delta_j) \tag{3.2.32}$$

$$\frac{\partial Q_\ell}{\partial V_i} = -2V_i\, y_{t_{ij}} \sin(-\Theta_{t_{ii}}) - \sum_{\substack{j=1\\ j\neq i}}^{g} y_{t_{ij}}\, V_j \sin(\delta_i - \Theta_{t_{ij}} - \delta_j) \tag{3.2.33}$$

$$\frac{\partial Q_\ell}{\partial V_j} = -V_i\, y_{t_{ij}} \sin(\delta_i - \Theta_{t_{ij}} - \delta_j) \tag{3.2.34}$$

$$\frac{\partial T_\ell}{\partial \delta_i} = \sum_{\substack{j=1\\ j\neq 1}}^{g} V_i\, y_{m_{ij}}\, V_j \sin(\delta_i - \Theta_{m_{ij}} - \delta_j) \tag{3.2.35}$$

$$\frac{\partial T_\ell}{\partial \delta_j} = -V_i\, y_{m_{ij}}\, V_j \sin(\delta_i - \Theta_{m_{ij}} - \delta_j) \tag{3.2.36}$$

$$\frac{\partial T_\ell}{\partial V_i} = -2V_i\, y_{m_{ii}} \cos(-\Theta_{m_{ii}}) - \sum_{\substack{j=1\\ j\neq 1}}^{g} y_{m_{ij}}\, V_j \cos(\delta_i - \Theta_{m_{ij}} - \delta_j) \tag{3.2.37}$$

$$\frac{\partial T_\ell}{\partial V_j} = -V_i\, y_{m_{ij}} \cos(\delta_i - \Theta_{m_{ij}} - \delta_j) \tag{3.2.38}$$

$$\frac{\partial U_\ell}{\partial \delta_i} = -\sum_{\substack{j=1\\ j\neq 1}}^{g} V_i\, Y_{m_{ij}}\, V_j \cos(\delta_i - \Theta_{m_{ij}} - \delta_j) \tag{3.2.39}$$

$$\frac{\partial U_\ell}{\partial \delta_j} = V_i\, y_{m_{ij}}\, V_j \cos(\delta_i - \Theta_{m_{ij}} - \delta_j) \tag{3.2.40}$$

$$\frac{\partial U_\ell}{\partial V_i} = -2V_i\, y_{m_{ii}} \sin(-\Theta_{m_{ii}}) - \sum_{\substack{j=1\\ j\neq 1}}^{g} y_{m_{ij}}\, V_j \sin(\delta_i - \Theta_{m_{ij}} - \delta_j) \tag{3.2.41}$$

$$\frac{\partial U_\ell}{\partial V_j} = -V_i\, y_{m_{ij}} \sin(\delta_i - \Theta_{m_{ij}} - \delta_j) \tag{3.2.42}$$

$$\frac{\partial E_\ell}{\partial \delta_i} = 0 \tag{3.2.43}$$

$$\frac{\partial E_\ell}{\partial \delta_j} = 0 \tag{3.2.44}$$

$$\frac{\partial E_\ell}{\partial V_i} = 1 \tag{3.2.45}$$

$$\frac{\partial E_\ell}{\partial V_j} = 0 \tag{3.2.46}$$

The equations given in this section yield the entries of estimator model $\underline{f}$ and the Jacobian F; thus, the iterative estimator algorithm, Eq. (3.1.10), can be used to determine the state estimate.

3.3 Example State Estimates

The example state estimates offered in this section serve to demonstrate the estimator formulation, of Sec. 3.2, when applied to two simple power systems. The estimator formulation is intended to find principle application with power systems containing both topological and load imbalances.

As yet, the available literature offers no analysis of topologically unbalanced power systems suitable to serve as a benchmark against which the estimator formulation can be compared. Hence, Example 1 applies the formulation to a well studied balanced power system. This example seeks to demonstrate that, in the absence of noise error, the state estimate resulting from the estimator formulation of Sec. 3.2 is identically equal to a base case loadflow solution obtained using conventional modeling and loadflow techniques.

Example 2 demonstrates the estimator formulation for a hypothetical power system containing both topological and load imbalances.

The iterative algorithm of Eq. 3.1.10 has been encoded as a WATFIV computer program. This program requires as input: (1) the admittance matrix Y_{t_R}, (2) the admittance matrix Y_{m_R}, (3) a set of measured variables $\underline{z}$, (4) an initial state $\underline{x}_o$, (5) a weighting matrix W, (6) a convergence tolerance $\underline{a}$, and (7) pointer arrays identifying estimator variables and ports. The program outputs the state estimate. The WATFIV source program employs an IMSL subprogram, LLSQF, made available through the Virginia Tech Computing Center.[30]

A listing of the WATFIV source program is available upon request through the Energy Research Group at Virginia Polytechnic Institute and State University.

Example 1

Consider the simple power system shown in Fig. 3.3.1. This balanced system is a variation of the well known Ward-Hale system.[31] Inasmuch as the system is balanced (load and topology), it can be represented by its positive sequence network. The system consists of six (6) buses, seven (7) line, two (2) transformers, two (2) sources, and three (3) complex loads.

All lines are modeled as equivalent Π networks. Lines connected to transformers are modeled such that a single equivalent Π network represents both line and transformer.[32] Thus, the primitive network (system sources and loads excluded) is represented as the set of per-unit admittances, not mutually coupled, shown in Fig. 3.3.2.

A base case loadflow solution for the system of Fig. 3.3.1 was determined using a Newton-Raphson algorithm. Bus 1 was specified as

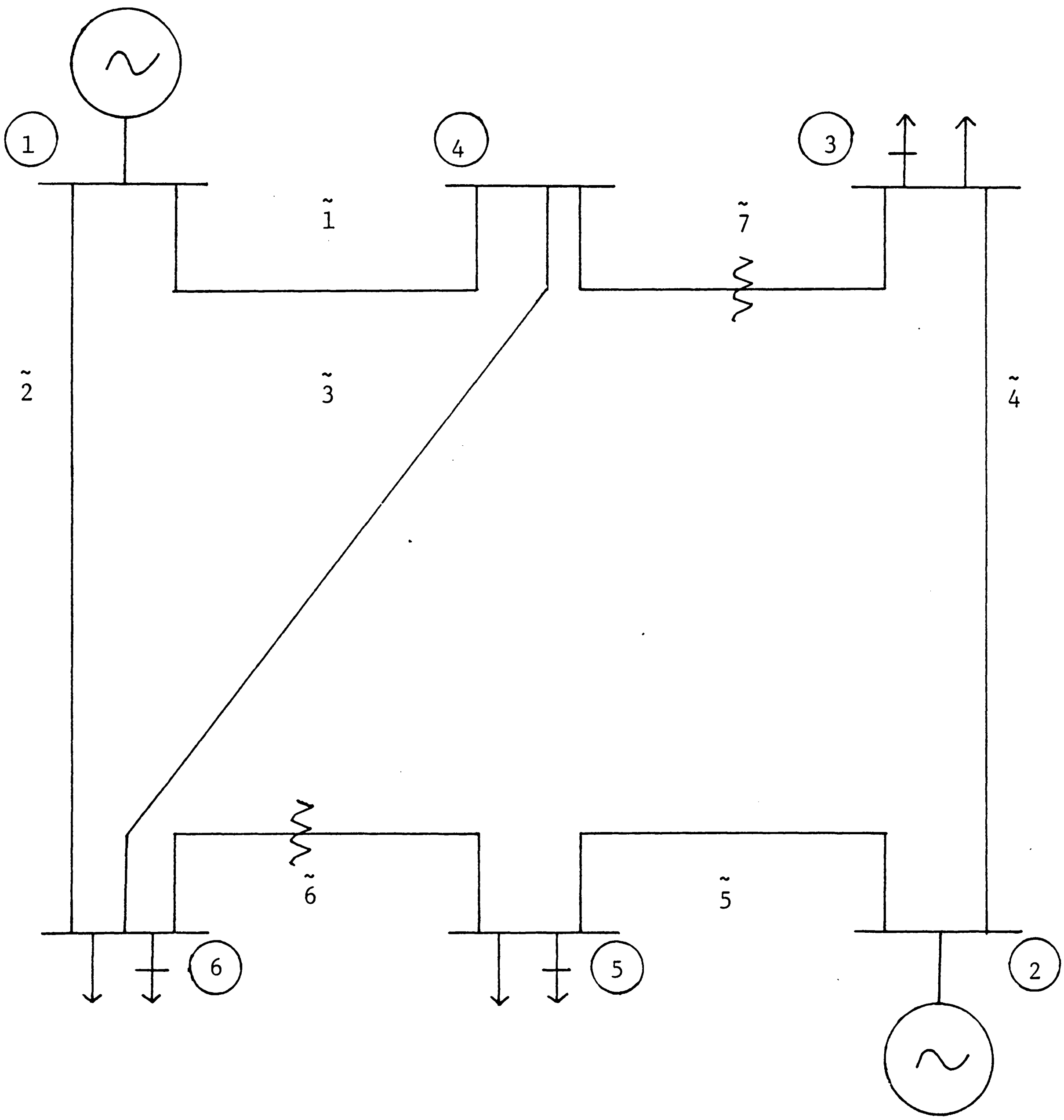

Fig. 3.3.1. One line diagram of a simple balanced power system.

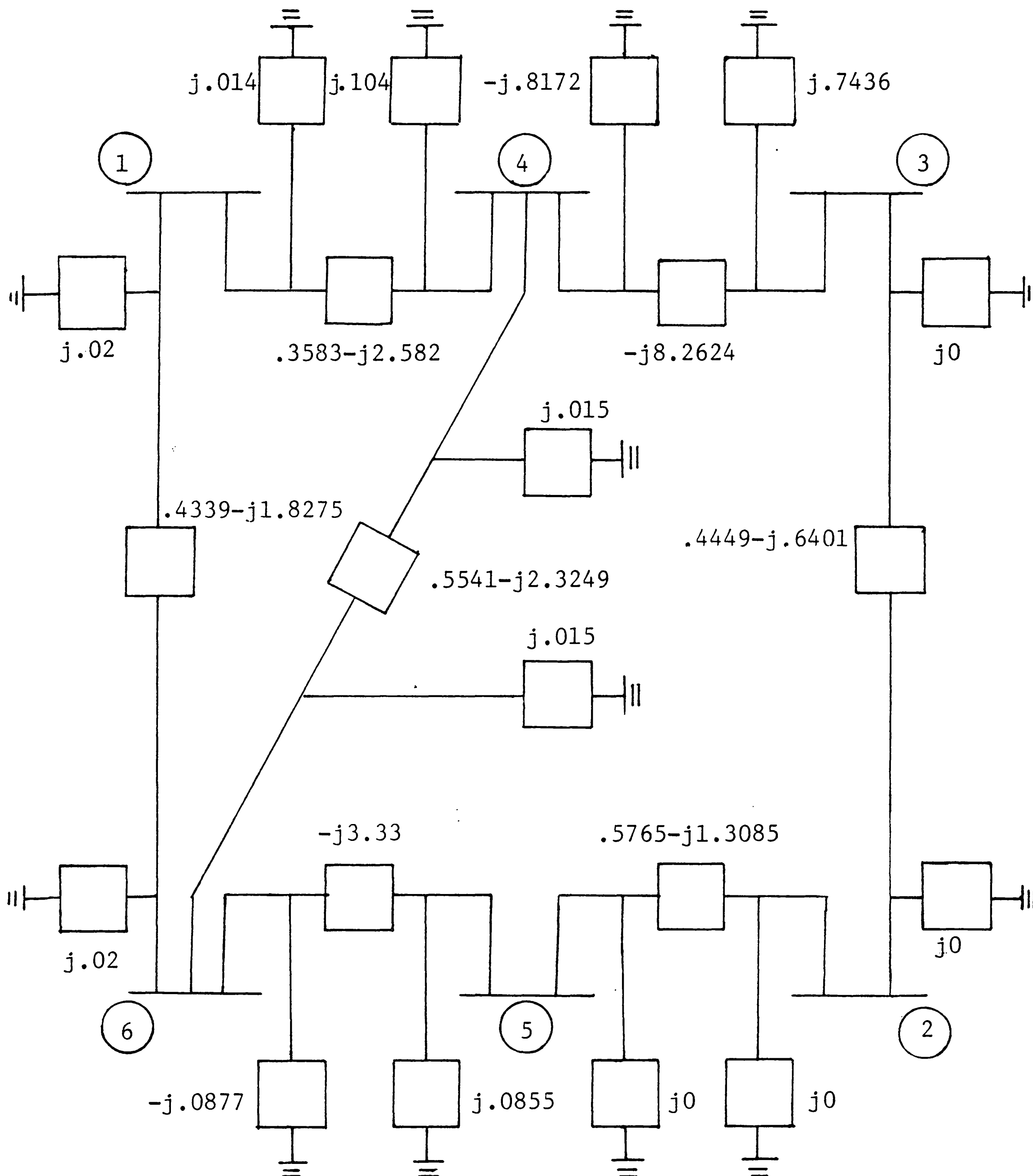

Fig. 3.3.2. Primitive network admittances.

the slack bus and line flows were calculated by Eq. 1.2.1. The per-unit loadflow solution is given in Table 3.3.1.

A directed graph representing the balanced system's primitive network is shown in Fig. 3.3.3. Node 0 is taken as the common ground node. The primitive network can be broken into seven (7) segments, one segment corresponding to each equivalent Π network.

Each equivalent Π can be replaced by its modified segment primitive. The presence of a common ground, node 0, indicates that no ground ports exist. All phase twigs are incident to the ground. The modified primitive network and system measurement tree are shown in Fig. 3.3.4. Darkened branches indicate twigs.

The complex power of any modified segment branch corresponds to a system complex line flow. The complex power of any system measurement twig corresponds to either system load or generation. This situation suggests that the estimator formulation of Sec. 3.2 can be used to obtain a system state estimate.

Let the measured variables $\underline{z}$ be given by the base case loadflow solution of Table 3.3.1; hence, the vector of measurement noise $\underline{\varepsilon}$ is identically zero. Measured variables are selected such that the system is observable. All bus voltages are state variables.

System port 1 corresponding to twig 1 of Fig. 3.3.4 is taken as the swing port; thus, the voltage across port 1 is assumed known. The absence of measurement noise suggests that the best estimate of the system state must be given by the bus voltages of the base case loadflow.

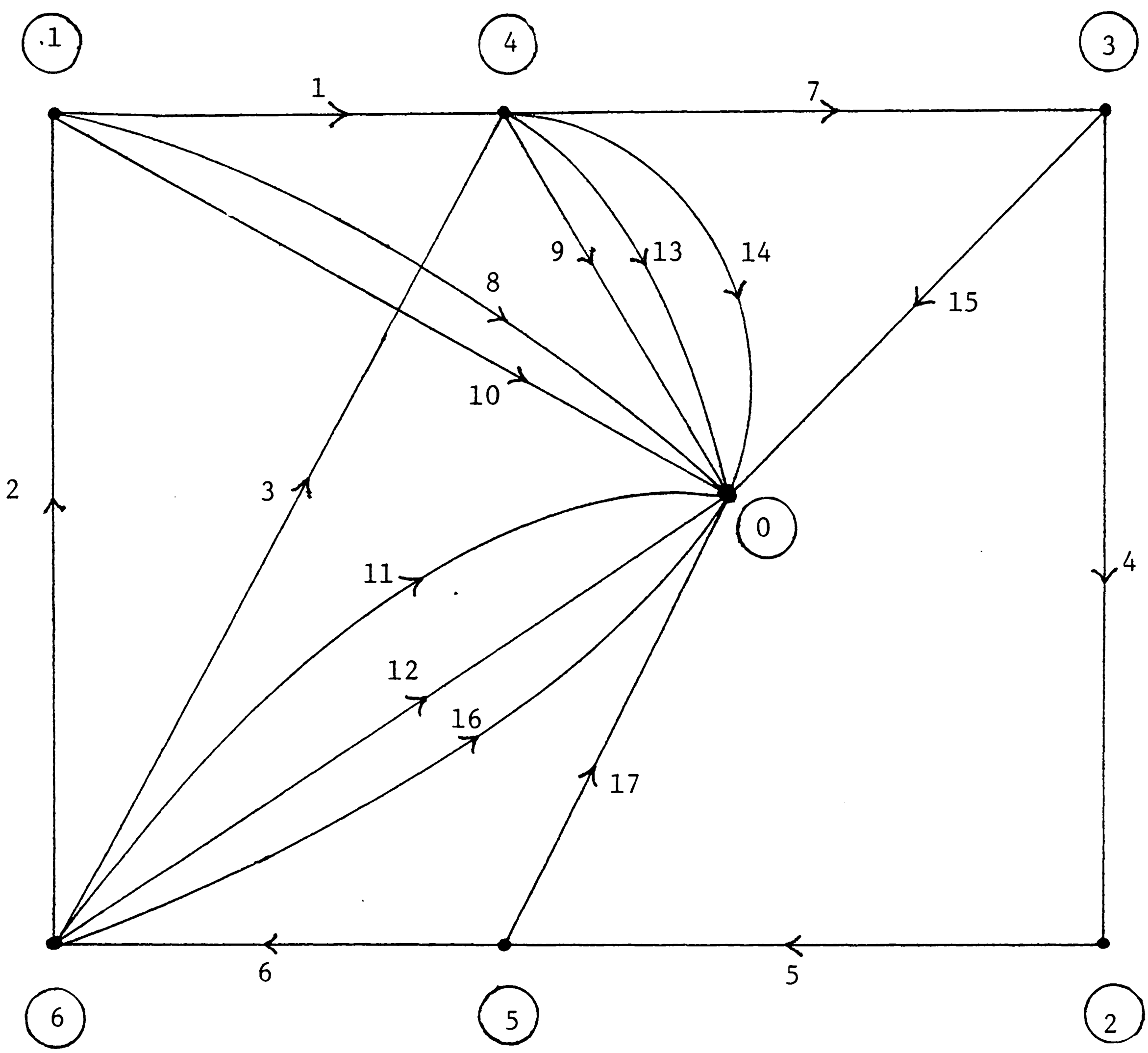

Fig. 3.3.3. Directed graph of system primitive network.

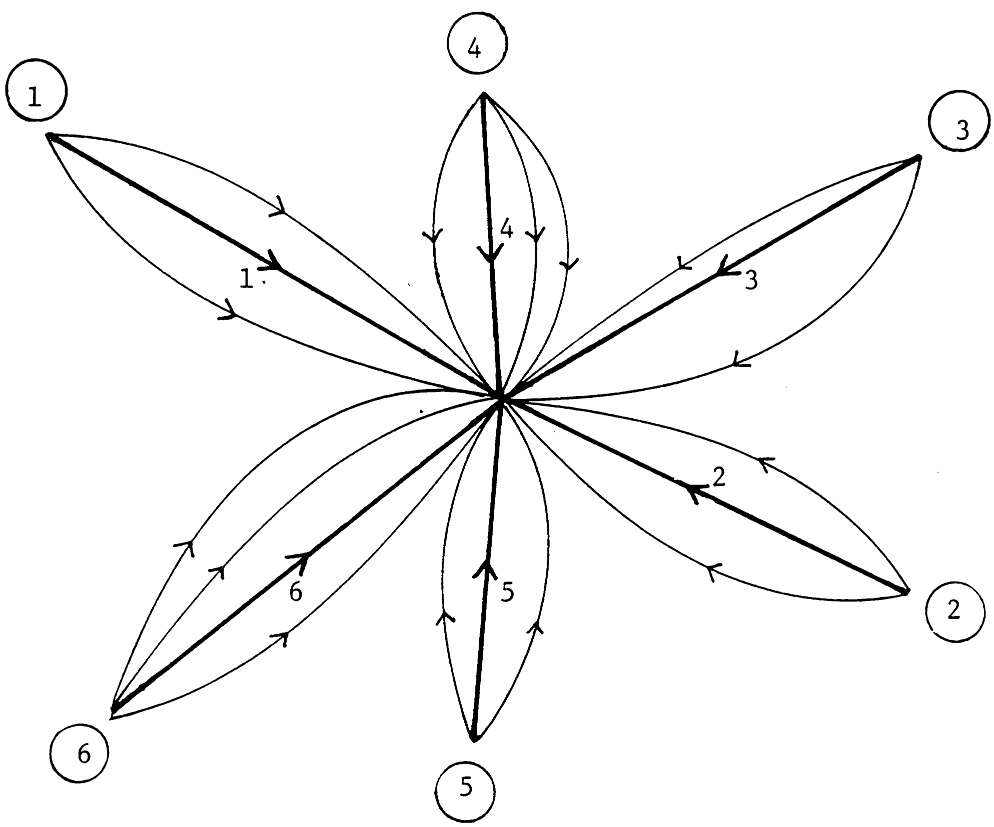

Fig. 3.3.4. Modified primitive network.

Table 3.3.1. Loadflow solution of simple balanced system.

BUS	V	δ°	P	Q	TO BUS	T	U
1	1.050	0.0	-0.951	-0.435			
					4	0.508	0.254
					6	0.442	0.180
2	1.100	-3.3	-0.500	-0.185			
					3	0.172	0.000
					5	0.328	0.184
3	0.999	-12.7	0.550	0.130			
					2	-0.154	0.024
					4	-0.395	-0.154
4	0.929	-9.8	0.000	0.000			
					1	-0.484	-0.170
					3	0.395	0.178
					6	0.089	-0.008
5	0.919	-12.3	0.300	0.180			
					2	-0.295	-0.109
					6	-0.004	-0.070
6	0.919	-12.2	0.500	0.050			
					1	-0.416	-0.107
					4	-0.088	-0.013
					5	0.004	0.071

The system state estimate was calculated using the algorithm of Eq. 3.1.10. The per-unit results of the state calculation are shown in Table 3.3.2. Note that system port numbers correspond directly to system bus numbers. The best estimates of all measured variables are given by $\underline{f}(\hat{\underline{x}})$.

The results shown in Table 3.3.2 indicate that the state estimate $\hat{\underline{x}}$ converges to the true state $\underline{x}$. Thus, in the absence of measurement noise, the estimator formulation of Sec. 3.2 yields the independently obtained loadflow solution.

Example 2

Consider the hypothetical unbalanced distribution feeder shown in Fig. 3.3.5. [33] Let the primary of the Δ-Y transformer bank be connected to an infinite bus at rated line-to-ground voltage. The feeder is considered an unbalanced power system.

Data describing feeder components is given as follows.

Transformer Data

Δ-Y Bank		115KV rated primary voltage 7.2KV rated secondary voltage 5MVA bank rated power z_t = 7% transformer impedance on rating
Open Y-Open Δ Bank	Unit I	7.2KV rated primary voltage 120/240V rated secondary voltage 50KVA unit rated power z_t = (1.1+j1.7)% transformer impedance on unit rating
	Unit II	7.2KV rated primary voltage 120/240V rated secondary voltage 15KVA unit rated power z_t = (1.3+j1.2)% transformer impedance on unit rating.

Table 3.3.2. State estimate results.

P-MEASUREMENTS

Port Number	Actual P	Measured P	Estimated P
1	-0.951	-0.951	-0.951
2	-0.500	-0.500	-0.500
3	0.550	0.550	0.550
4	0.000	0.000	0.000
5	0.300	0.300	0.300
6	0.500	0.500	0.500

Q-MEASUREMENTS

Port Number	Actual Q	Measured Q	Estimated Q
1	-0.435	-0.435	-0.435
2	-0.185	-0.185	-0.185
3	0.130	0.130	0.130
4	0.000	0.000	0.000
5	0.180	0.180	0.180
6	0.050	0.050	0.050

T-MEASUREMENTS

From Port	To Port	Actual T	Measured T	Estimated T
1	4	0.508	0.508	0.508
3	2	-0.154	-0.154	-0.154
5	6	-0.004	-0.004	-0.004
3	4	-0.395	-0.395	-0.395
4	3	0.395	0.395	0.395
6	1	-0.416	-0.416	-0.416

U-MEASUREMENTS

From Port	To Port	Actual U	Measured U	Estimated U
1	4	0.254	0.254	0.254
3	2	0.024	0.024	0.024
5	6	-0.070	-0.070	-0.070
3	4	-0.154	-0.154	-0.154
4	3	0.178	0.178	0.178
6	1	-0.107	-0.107	-0.107

Table 3.3.2. State estimate results (Continued).

E-MEASUREMENTS

Port Number	Actual E	Measured E	Estimated E
2	1.100	1.100	1.100
3	0.999	0.999	0.999
4	0.929	0.929	0.929
5	0.919	0.919	0.919
6	0.919	0.919	0.919

STATE VARIABLES

Port Number	Actual V	Actual δ	Estimated V	Estimated δ
1	1.05	0.0	1.05	0.0
2	1.100	-3.3	1.100	-3.3
3	0.999	-12.7	0.999	-12.7
4	0.929	-9.8	0.929	-9.8
5	0.919	-12.3	0.919	-12.3
6	0.919	-12.2	0.919	-12.2

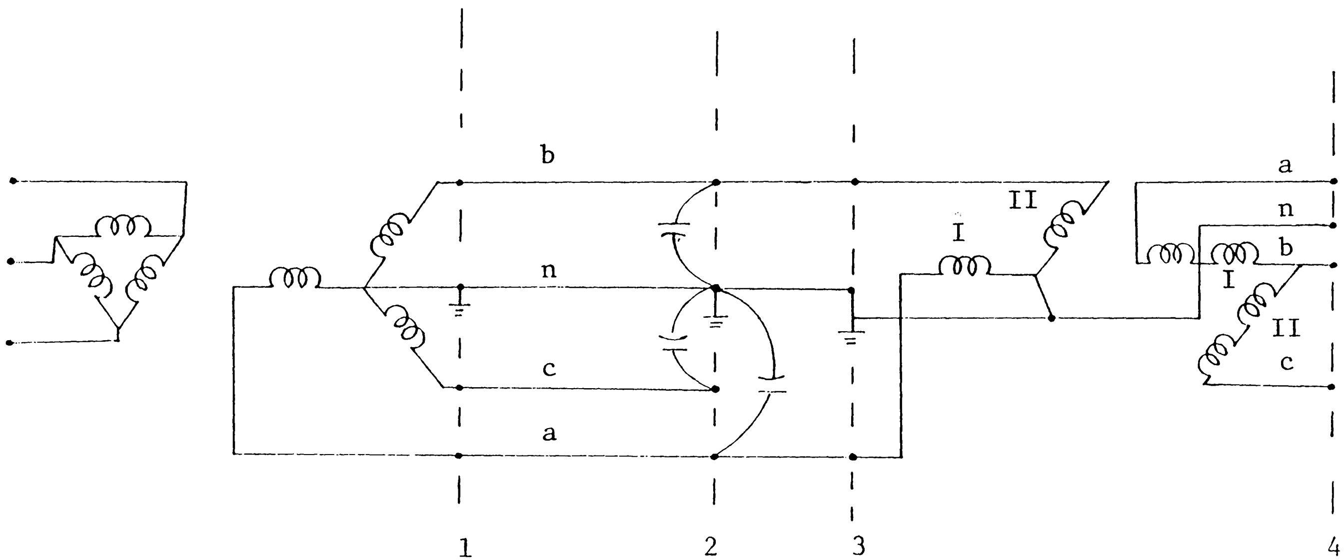

Fig. 3.3.5. Unbalanced distribution feeder.

Fixed Capacitor Data

Y-Capacitor Bank at 2	y_c (phase a) = $j9.645\times10^{-4}$ v
	y_c (phase b) = $j9.645\times10^{-4}$ v
	y_c (phase c) = $j9.645\times10^{-4}$ v

Conductor Data

3-ϕ line from 1 to 2	4.3 miles (line length) 4/0 ACSR (phase conductors) 1/0 ACSR (neutral conductor) Conductor spacing is shown in Fig. 3.3.6a
2-ϕ line from 2 to 3	7.8 miles (line length) 1/0 ACSR (phase conductors) 1/0 ACSR (neutral conductors) Conductor spacing is shown in Fig. 3.3.6b.

Neutral conductors of the unbalanced feeder are grounded to the earth's surface. The earth's surface is assumed to have a resistivity of 100 Ω-meters.[23] All system loads are connected phase to neutral. The infinite bus is represented as a balanced, 3-ϕ, wye-connected voltage source with solidly grounded neutral.

When the transformer banks are represented by transformer primitive branches, the feeder is represented by the directed graph shown in Fig. 3.3.7. For clarity, branches representing conductor distributed capacitance effects are not shown in Fig. 3.3.7.

The unbalanced feeder consists of five (5) segments: two (2) conductor segments, two (2) transformer segments, and one (1) auxiliary device segment (capacitor bank). The modified primitive network and system measurement tree are shown in Fig. 3.3.8. Darkened branches indicate measurement twigs.

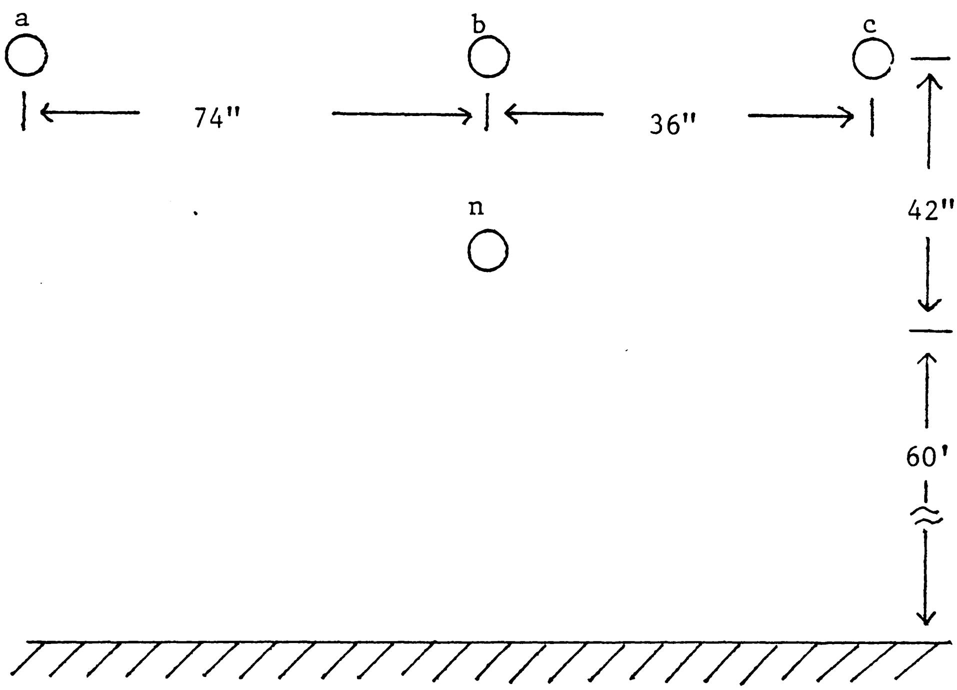

Fig. 3.3.6a. Conductor spacing of 3-ϕ line.

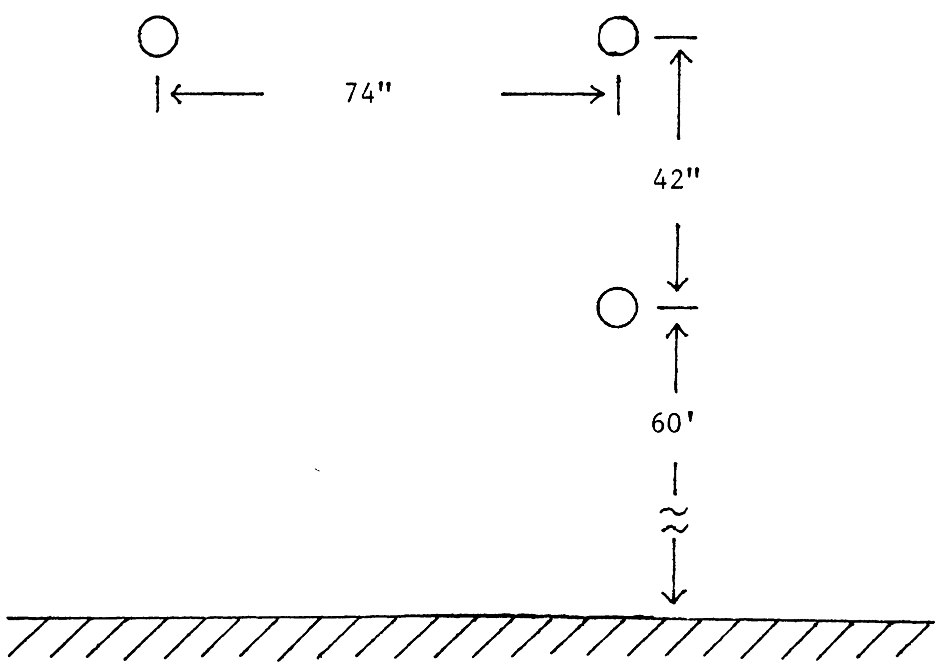

Fig. 3.3.6b. Conductor spacing of 2-ϕ line.

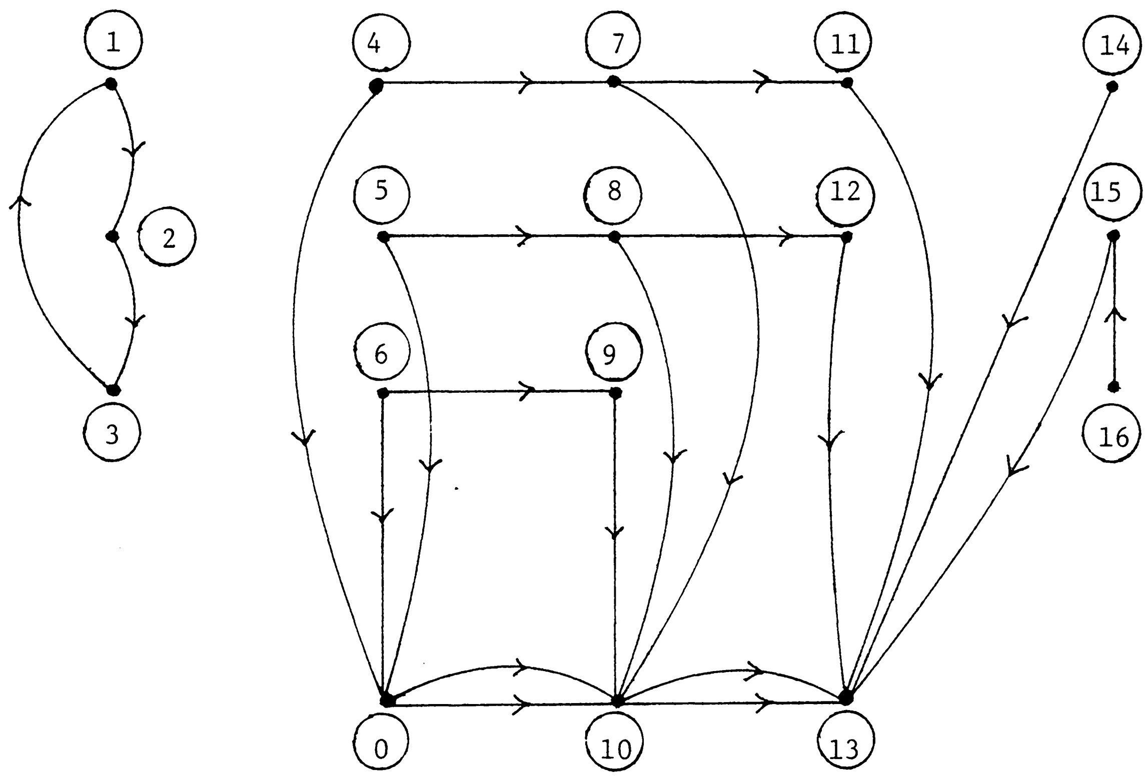

Fig. 3.3.7. Primitive network of the unbalanced feeder.

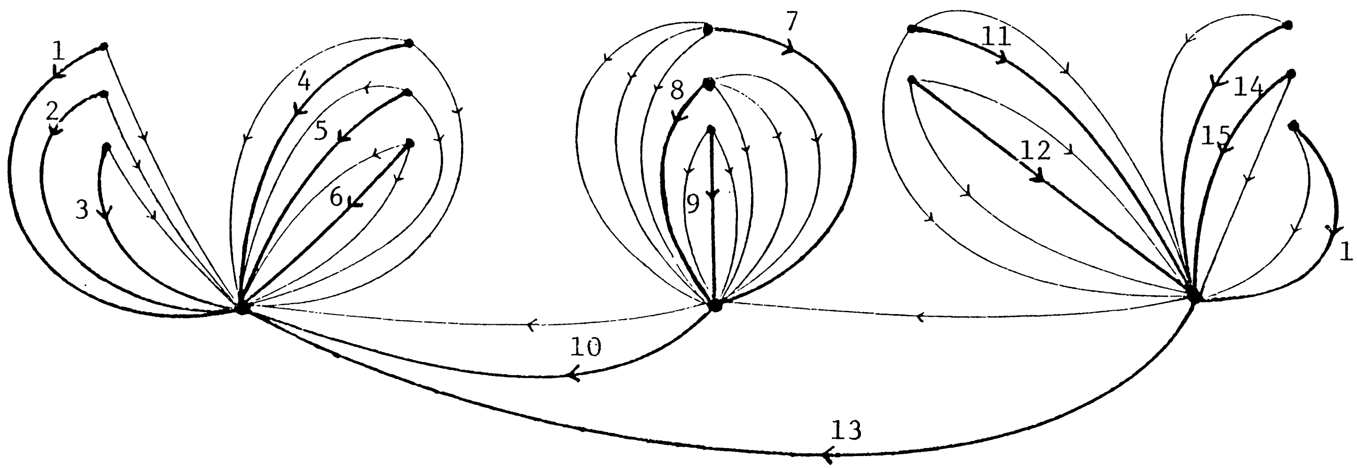

Fig. 3.3.8. Modified primitive network and measurement tree.

A computer program to calculate the Y_{t_R} and Y_{m_R} admittance matrices for a class of unbalanced power systems has been developed[1]. Power systems given as input to the program must be such that all unbalanced sources and loads are connected phase to ground.[34] A program source listing is made available through the Energy Research Group at Virginia Polytechnic Institute and State University.

The unbalanced feeder of Fig. 3.3.5 is of the class of systems acceptable as input to the aforementioned computer program. The Y_{t_R} and Y_{m_R} admittance matrices of the unbalanced feeder were calculated.

A set of measured variables was selected for the system and the corresponding state variables identified. Hypothetical system loads were assumed. Using the Y_{t_R} and Y_{t_m} admittance matrices, a base case load flow solution of the unbalanced feeder was determined. Ports 1, 2, and 3 were taken as the slack ports.

Hypothetical measurements were obtained by introducing error to system variables given by the base case loadflow.. A diagonal estimator weighting matrix W was heuristically selected such that: (1) all load measurements were weighted 1.0, (2) all conductor flow measurements were weighted 0.25, and (3) all phase voltage magnitude measurements were weighted 0.10.

The system state estimate was calculated using the algorithm of Eq. 3.1.10. Ports 1, 2, and 3 were taken as swing ports; thus, their voltages were known deterministically. The results of the state

---

[1] Computer program was developed by D. L. Allen under sponsorship of the Energy Research Group at Virginia Polytechnic Institute and State Univ.

calculation, given in real units, are shown in Table 3.3.3. The best estimates of all measured variables are given by $\underline{f}(\hat{\underline{x}})$.

The results displayed in Table 3.3.3 indicate that the estimator formulation of Sec. 3.2 yields a reasonable estimate of the true system state when applied to a topologically unbalanced power system. These results are only intended to demonstrate convergence to an acceptable result.

Inasmuch as analysis of the estimator quality is considered beyond the scope of this dissertation, accuracy of any given state estimate is not considered.

Table 3.3.3. State calculation results.

P-MEASUREMENTS

Port Number	Actual P(KW)	Measured P(KW)	Estimated P(KW)
4	200.000	198.500	198.784
5	200.000	199.500	197.745
6	200.000	199.000	198.903
7	30.000	30.500	30.277
8	30.000	30.000	29.771
9	30.000	29.500	30.851
11	0.000	0.000	-0.032
12	0.000	0.500	0.173
14	20.000	20.000	19.608
15	20.000	19.500	19.615
16	20.000	20.500	19.169

Q-MEASUREMENTS

Port Number	Actual Q-(KVAR)	Measured Q (KVAR)	Estimated Q (KVAR)
4	300.000	300.000	300.001
5	300.000	295.000	297.290
6	300.000	304.000	299.997
7	60.000	59.500	60.323
8	60.000	60.000	59.356
9	60.000	59.500	59.085
11	0.000	0.500	0.830
12	0.000	0.000	-0.665
14	15.000	15.500	14.289
15	15.000	15.000	14.304
16	15.000	14.500	16.083

Table 3.3.3. State calculations results (Continued).

T-MEASUREMENTS

From Port	To Port	Actual T(KW)	Measured T(KW)	Estimated T(KW)
4	7	60.570	60.500	60.080
5	8	64.331	64.000	61.879
6	9	30.286	30.000	30.694
7	4	-60.001	-60.000	-60.020
8	5	-63.088	-63.000	-61.024
9	6	-30.203	-30.000	-30.884

U-MEASUREMENTS

From Port	To Port	Actual U(KVAR)	Measured U(KVAR)	Estimated U(KVAR)
4	7	17.561	17.500	19.980
5	8	59.135	59.000	55.025
6	9	10.550	10.500	10.200
7	4	-16.031	-16.000	-19.253
8	5	-57.507	-58.000	-54.907
9	6	-10.522	-10.500	-10.209

E-MEASUREMENTS

Port Number	Actual E(KV)	Measured E(KV)	Estimated E(KV)
11	7.018	7.018	7.009
12	6.829	6.820	6.850

Table 3.3.3. State calculation results (Continued).

STATE VARIABLES

Port Number	Actual V(KV)	Actual (deg.)	Estimated V(KV)	Estimated (deg.)
5	7.089	119.352	7.091	119.359
4	7.103	-0.633	7.102	-0.630
6	7.104	-120.558	7.105	-120.557
8	6.993	119.502	7.001	119.503
7	7.068	-1.218	7.064	-1.175
9	7.139	-120.476	7.137	-120.512
16	0.191	-155.326	0.191	-154.874
12	6.829	120.147	6.847	120.121
11	7.018	-2.148	7.010	-2.034
15	0.106	-60.719	0.107	-60.663
14	0.108	118.276	0.109	118.297
1	66.401	90.000	66.401	90.000
2	66.401	-30.000	66.401	-30.000
3	66.401	-150.000	66.401	-150.000

CHAPTER 4. CONCLUSIONS AND RECOMMENDATIONS FOR FURTHER RESEARCH

State estimation of power systems has, until now, been limited to balanced systems which can be represented by positive sequence networks. The available literature offers no treatment of state estimation of unbalanced power systems.

State estimation of unbalanced power systems must rely on accurate network models representing power systems containing both topological and load imbalances. The available literature offers no such models.

4.1 Conclusions

A new network model has been developed which allows the calculation of state estimates for a class of unbalanced power systems. This model is applicable to systems which exhibit both topological and load imbalances.

The network model, representing power systems operating in steady state, yields a set of complex algebraic equations in variables convenient for an accepted state estimation technique. Development of the model equations appeal to multiport network theory and graph theoretic principles.

The general methodology for obtaining multiport equations for admittance networks has been presented. The general methodology demonstrates port identification via imposition of a measurement tree.

Multiport equations for unbalanced power systems have been developed in two stages. First, the concept of power system segments has been introduced. Rules have been established for decomposing power systems into segments. The general methodology allows the formulation of segment multiport equations.

The decomposition of power systems into segments is a new concept which allows the formulation of equations which give conductor power flows as a function of voltages in the phase voltage reference frame. Rules for selecting segment measurement trees have been given such that segment port variables correspond to measured and state variables needed for state estimation.

The second stage of developing power system multiport equations requires a scheme to examine the topology of interconnected power system segments. The concept of replacing segment primitives with <u>modified</u> segment primitives has been introduced. The union of all modified segment primitives forms a modified primitive network.

The modified primitive network is a new concept which allows the passive components of an unbalanced power system to be represented by an equivalent multiport network. Rules for selecting a system measurement tree for the modified primitive network have been given such that system port variables correspond to measured and state variables.

The general methodology for obtaining multiport equations for admittance networks can be applied to the modified primitive network with a system measurement tree specified. The methodology yields equations which give system loads as a function of voltages in the phase voltage reference frame.

Linear dependence among multiport equations has been examined. Topological dependence and dependence among primitive equations has been considered. Normalization of multiport equations has been examined and a scheme to obtain per-unit segment primitive equations is described.

State estimation of unbalanced power systems appeals to the extended method of weighted least squares. An iterative algorithm to determine the least squares estimate has been presented.

Rules are established which identify necessary state voltages for unbalanced power systems. Estimator equations are formulated from the multiport equations of the new network model. The concept of port suppression is developed as a method to obtain estimator equations as a function of state variables only.

Two examples have been offered that demonstrate the estimator formulation. Example 1 considers the formulation when applied to a well studied balanced power system. Example 2 demonstrates the estimator formulation for a hypothetical unbalanced power system. The resulting state estimates demonstrate that the new network model can be employed to formulate a state estimator for power systems exhibiting both topological and load imbalances.

4.2 Recommendations for Further Research

State estimation of unbalanced power systems will likely find broadest application in the lower voltage (13.5 KV and below) distribution systems. Rapid load variations are characteristic of power distribution systems; hence, state estimates for such systems must be updated rapidly. A typical distribution system can consist of hundreds of nodes. It is essential that state estimate computation time be minimized.

The voltage profile of a typical distribution system can vary greatly over time. Per-unit voltage magnitudes can vary by more than ten percent at some nodes. Per-unit load powers can differ by several orders of magnitude. These considerations suggest that any practical state estimator must be robust.

Experienced gained with the iterative algorithm of Eq. (3.1.10) has shown that the convergence rate of the algorithm is sensitive to: (1) the number of redundant measurements (m-n), (2) the initial state $\underline{x}_o$ (starting voltage profile), and (3) the weighting matrix W.

Three areas for research directed towards the practical application of state estimators for unbalanced systems will be discussed: (1) normalization of multiport equations, (2) distributed state estimation, and (3) recursive weighted least squares.

Normalization of Multiport Equations

The normalization scheme offered in Sec. 2.4 is a natural extension of normalization of balanced power systems. This scheme requires a real base voltage for each segment and a real system base power.

Base voltages are most often chosen to be a segment phase-to-neutral nominal voltage magnitude.

Often unbalanced systems contain segments having corresponding phase ports with unequal nominal phase-to-neutral voltage magnitudes. Hence, corresponding phase port voltages, in per-unit, may differ greatly. Clearly, the initial state $\underline{x}_o$ (starting voltage profile) for the algorithm of Eq. 3.1.10 must be carefully specified so as to agree with the per-unit scheme.

Additional research directed towards normalization of segment multiport equations is recommended. The following per-unit transformation is suggested.

Let the segment multiport equations be given in real units as

$$-\underline{I}_m = Y_m \, \underline{V}_m \qquad (4.2.1)$$

Define segment per-unit currents and voltages as

$$\underline{I}_{m_{pu}} = \frac{1}{S_B^*} E_B^* \, \underline{I}_m \qquad (4.2.2)$$

$$\underline{V}_{m_{pu}} = E_B^{-1} \, \underline{V}_m \qquad (4.2.3)$$

where,

S_B = complex system base power

E_B = diagonal matrix of complex base port voltages.

It follows that

$$-\frac{1}{S_B^*} E_B^* \, \underline{I}_m = \frac{1}{S_B^*} E_B^* \, Y_m \, E_B \, E_B^{-1} \, \underline{V}_m \, . \qquad (4.2.4)$$

The per-unit segment multiport equations are given by

$$-\underline{I}_{m_{pu}} = Y_{m_{pu}} \underline{V}_{m_{pu}} \tag{4.2.5}$$

where,

$$Y_{m_{pu}} = \frac{1}{S_B^*} E_B^* Y_m E_B$$

The per-unit transformations of Eqs. (4.2.2) and (4.2.3) allow port voltage angles and magnitudes to be normalized.

Distributed State Estimation

Implementation of a state estimator in a large unbalanced system requires much computer storage capability. Computation time to determine the state estimate can be excessive. In large systems, measurements telemetered to a central computing facility can require telemetry channels many miles in length. Research directed towards distributed processing of state estimates is recommended.

Consider the arbitrary large system shown in Fig. 4.2.1. Let the system be arbitrarily divided into n overlapping subsystems so that each system component belongs to one or more subsystems.

The system multiport equations are given by

$$-\underline{I}_{t_R} = Y_{t_R} \underline{V}_{t_R} \tag{4.2.6}$$

Let each subsystem be considered as an independent system. Thus, multiport equations for the k^{th} subsystem can be determined and are given by

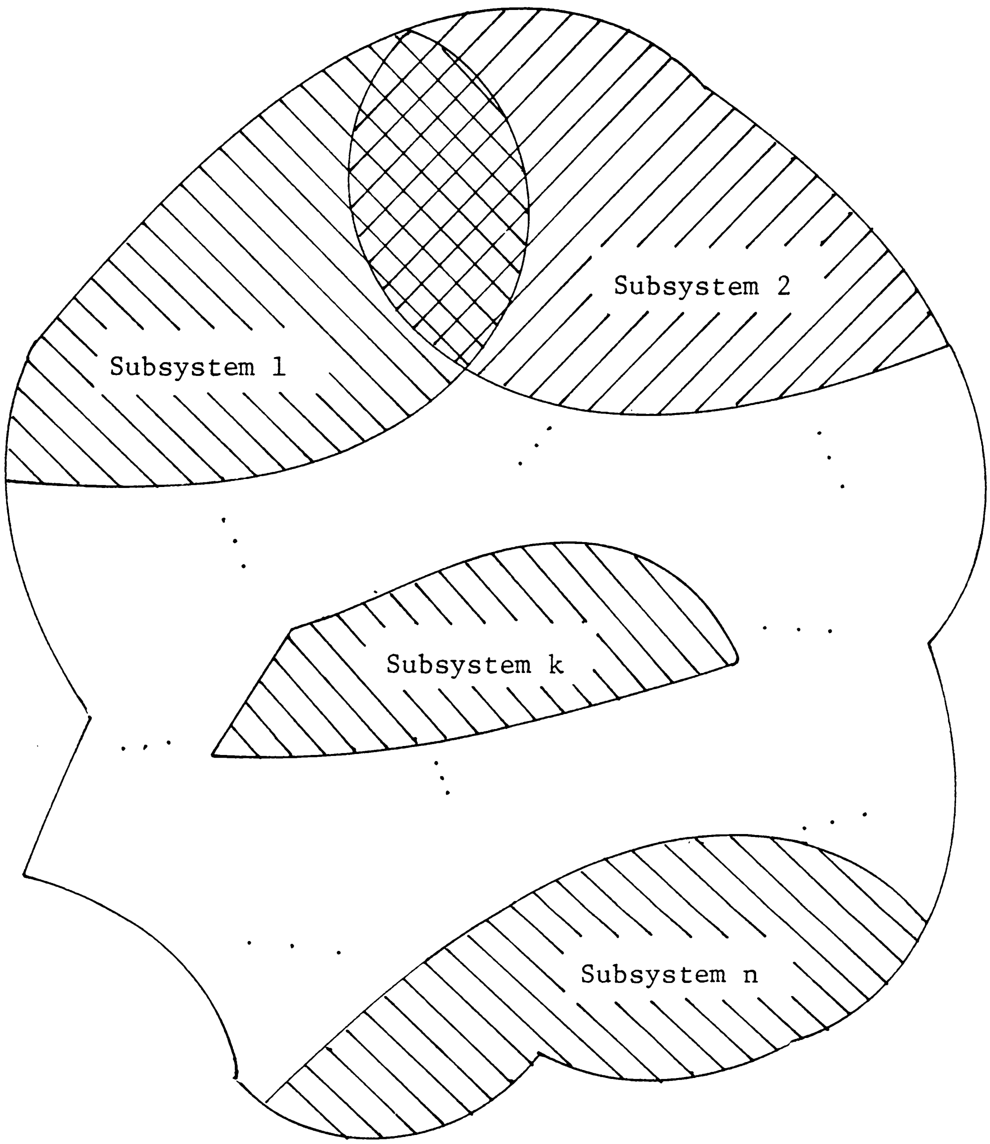

Fig. 4.2.1. Large system divided into overlapping subsystems.

$$\underline{I}_{t_{Rk}} = Y_{t_{Rk}} \underline{V}_{t_{RK}} \tag{4.2.7}$$

$$\underline{I}_{m_{Rk}} = Y_{m_{Rk}} \underline{V}_{m_{Rk}} \tag{4.2.8}$$

Let a state estimator, as developed in Chapter 3, be assigned to each subsystem. Assume measurements are available such that each subsystem is observable.

Given the conditions setforth above, a state estimate can be determined for each subsystem. The state estimate $\hat{\underline{x}}_k$ of the k^{th} subsystem determines that subsystems state voltages $\underline{V}_{t_{Rk}}$. The best estimate of the k^{th} subsystem's port currents $\hat{\underline{I}}_{t_{Rk}}$ is given by

$$\hat{\underline{I}}_{t_{Rk}} = Y_{t_{Rk}} \hat{\underline{V}}_{t_{Rk}} \tag{4.2.9}$$

From Eq. (4.2.9), the best estimate of subsystem port admittance can be determined. For the i^{th} port of the k^{th} subsystem, the best estimate of port admittance is given by

$$\hat{y}_{k_i} = \hat{I}_{t_{Rki}} / \hat{V}_{t_{Rki}} \tag{4.2.10}$$

where,

$\hat{y}_{k_i}$ = best estimate of load admittance at the i^{th} port

$\hat{I}_{t_{Rki}}$ = best estimate of the i^{th} port current

$\hat{V}_{t_{Rki}}$ = best estimate of the i^{th} port voltage.

Let the system multiport equations of Eq. (4.2.6) be partitioned such that

$$-\begin{bmatrix} \underline{I}_{t_{RS}} \\ \underline{I}_{t_{RL}} \end{bmatrix} = \begin{bmatrix} Y_{t_{SS}} & Y_{t_{SL}} \\ Y_{t_{LS}} & Y_{t_{LL}} \end{bmatrix} \begin{bmatrix} \underline{V}_{t_{RS}} \\ \underline{V}_{t_{RL}} \end{bmatrix} \qquad (4.2.11)$$

where,

$\underline{I}_{t_{RS}}$ = vector of system reference port currents

$\underline{V}_{t_{RS}}$ = vector of system reference port voltages

$\underline{I}_{t_{RL}}$ = vector of system load port currents

$\underline{V}_{t_{RL}}$ = vector of system load port voltages.

Let the system reference port voltages $\underline{V}_{t_{RS}}$ be given. It remains to determine the load port voltages $\underline{V}_{t_{RL}}$, in order to obtain the system state.

From Eq. (4.2.10), it can be shown that

$$-\underline{I}_{t_{RL}} = Y_{t_{LS}} \underline{V}_{t_{RS}} + Y_{t_{LL}} \underline{V}_{t_{RL}} \qquad (4.2.12)$$

Each system load port can be found in one or more subsystems. Thus, the best estimate of system load port currents $\hat{\underline{I}}_{t_{RL}}$ can be written as

$$\hat{\underline{I}}_{t_{RL}} = \hat{Y}_L \underline{V}_{t_{RL}} \qquad (4.2.13)$$

where,

$\hat{Y}_L$ = diagonal admittance matrix with diagonal entries of $\hat{y}_{k_i}$.

Substituting $\hat{\underline{I}}_{t_{RL}}$ for $\underline{I}_{t_{RL}}$ in Eq. (4.2.12) suggests that the best estimate of load port voltages $\hat{\underline{V}}_{t_{RL}}$ can be obtained from

$$-\hat{Y}_L \hat{\underline{V}}_{t_{RL}} = Y_{t_{LS}} \underline{V}_{t_{RS}} + Y_{t_{LL}} \hat{\underline{V}}_{t_{RL}} \tag{4.2.14}$$

Solving Eq. (4.2.14) for $\hat{V}_{t_{RL}}$ yields

$$\hat{\underline{V}}_{t_{RL}} = =(\hat{Y}_L + Y_{t_{LL}})^{-1} Y_{t_{LS}} \underline{V}_{t_{RS}} \tag{4.2.15}$$

Equation (4.2.15) suggests that a state estimate can be obtained by estimating system port admittances. Estimates of system port admittances can be obtained from subsystem state estimates. The subsystem state estimates are computed independently and simultaneously in a distributed processing scenario. Research directed towards optimal subsystem identification is recommended.

Recursive Weighted Least Squares

Practical application of state estimators in distribution systems will likely require many load measurements in order to obtain observability. The availability of many load measurements suggests that recursive weighted least squares may offer a more time efficient and robust estimator than the formulation given by Eq. (3.1.10).

A recursive least squares estimator would begin with a loadflow solution obtained from only load measurements. Redundant conductor power flow measurements and phase voltage magnitude measurements would be processed into the state estimate recursively.

The state estimate would be obtained in a manner similar to extended Kalman Filtering.[35] Research directed towards development of recursive weighted least squares estimators for unbalanced systems is recommended.

REFERENCES

[1] J. F. Dopazo, O. A. Klitin, G. W. Stagg and L. S. Van Slyck, "State calculation of power system from line flow measurements", IEEE Trans. on Power Apparatus and Systems, vol. PAS-89, pp. 1698-1708, September/October 1970.

[2] J. F. Dopazo, O. A. Klitin and L. S. Van Slyck, "State calculation of power systems from line flow measurements, Part II", Ibid, vol. PAS-91, pp. 145-151, January/February 1972.

[3] F. C. Schweppe and J. Wildes, "Power system static-state estimation, Part I: exact model", Ibid, vol. PAS-89, pp. 120-125, January 1970.

[4] F. C. Schweppe and D. B. Rom, "Power system static-state estimation, Part II: approximate model", Ibid, pp. 125-130, January 1970.

[5] F. C. Schweppe, "Power system static-state estimation, Part III: implementation", Ibid, pp. 130-135, January 1970.

[6] R. E. Larson, W. F. Tinney and J. Peschon, "State estimation in power systems, Part I: theory and feasibility", Ibid, pp. 345-352, March 1970.

[7] R. E. Larson, W. F. Tinney, L. P. Hajdu and D. S. Piercy, "State estimation in power systems, Part II: implementation and applications", Ibid, pp. 353-363, March 1970.

[8] O. J. M. Smith, "Power system state estimation", Ibid, pp. 363-379, March 1970.

[9] A. S. Debs and R. E. Larson, "A dynamic estimator for tracking the state of a power system", Ibid, vol. PAS-89, pp. 1670-1677, September/October 1970.

[10] R. D. Masiello and F. C. Schweppe, "A tracking static-state estimator", Ibid, vol. PAS-90, pp. 1025-1033, May/June 1971.

[11] B. Porretta and R. S. Dhillon, "Performance evaluation of state estimation from line flow measurements on Ontario Hydro Power Systems", Ibid, vol. PAS-92, pp. 1696-1701, September/October 1973.

[12] J. F. Dopazo, et al, "Justification of AEP real time load flow project", Ibid, pp. 1501-1509.

[13] A. S. Debs, "Estimation of steady-state power system model parameters", Ibid, vol. PAS-93, pp. 1260-1268, September/ October 1974.

[14] K. Srinivasan and Y. Robichaud, "A dynamic estimator for complex bus voltage determination", Ibid, pp. 1581-1588.

[15] W. D. Stevenson, Elements of Power Systems Analysis, McGraw-Hill, New York, 1975.

[16] N. Balabanian and T. A. Bickert, Electrical Network Theory, Wiley, New York, 1969,

[17] G. A. Campbell, "Mutual impedances of grounded circuits", Bell System Technical Journal, Oct., 1923, pp. 1-30.

[18] O. Mayr, "Einphasiger erdschluss und doppelerdschluss in vermaschten leitungsnetzen", Archiv für Elektrotecknik, V. 17, Oct. 1926, pp. 163-173.

[19] J. R. Carson, "Wave propagation in overhead wires with ground return", The Bell System Technical Journal, V. 5, Oct. 1926, pp. 539-554.

[20] C. F. Wagner and R. D. Evans, Symmetrical Components", McGraw-Hill, New York, 1933.

[21] C. A. Gross, Power Systems Analysis, John Wiley and Sons, New York, 1979.

[22] P. Lorrain and D. Corson, Electromagnetic Fields and Waves, W. H. Freeman and Co., San Francisco, 1970.

[23] P. M. Anderson, Analysis of Faulted Power Systems, Iowa State Univ. Press, Ames, 1973.

[24] N. A. Demerdash, "Transients in power systems", Unpublished lecture notes, Virginia Polytechnic Institute and State University, 1976.

[25] W. A. Lewis, G. D. Allen and A. B. Chance, "Symmetrical-component circuit constants and neutral circulating currents for concentric-neutral underground distribution cables", IEEE Trans. on Power Apparatus and Systems, vol. PAS-97, pp. 191-207, Jan./Feb. 1978.

[26] W. K. Chen, Applied Graph Theory Graphs and Electrical Networks, North Holland Publishing Co., New York, 1976.

[27] B. Nobel, Applied Linear Algebra, Prentice-Hall, Inc., Englewood Cliffs, NJ, 1969.

[28] D. M. Simmons, Nonlinear Programming for Operations Research, Prentice-Hall, Inc., Englewood Cliffs, NJ, 1975.

[29] J. Konenta, Elements of Econometrics, Macmillan Publishing Co., Inc., New York, 1971.

[30] International Mathematics and Statistics Library, "The IMSL library vol. 1", IMSL, Inc., Houston, 1980.

[31] J. B. Ward and H. W. Hale, "Digital computer solution of power flow problems", Trans. AIEE, V. 75, Part 3, June, 1956, pp. 398-404.

[32] G. W. Stagg and A. H. El-Abiad, Computer Methods in Power System Analysis, McGraw-Hill, New York, 1968.

[33] L. R. Herman, "Typical unbalanced distribution feeder", Unpublished lecture notes, North Carolina State University, 1978.

[34] D. L. Allen, "Multireference power system modeling and multi-phase load flow analysis", Ph.D. Dissertation, Virginia Poly-Technic Institute and State University, 1982.

[35] W. L. Brogan, Modern Control Theory, Quantum Publishers, Inc., New York, 1974.

APPENDIX A. Y_{BUS} FROM THE GENERAL METHODOLOGY

It is known from network theory that the nodal admittance matrix Y_{BUS} is given by

$$Y_{BUS} = A_\ell \, Y_\ell \, A_\ell^T \tag{A.1}$$

It follows from Eq. (2.1.3) that

$$B_t^T = -Q_\ell \tag{A.2}$$

It follows from Eq. (2.1.4) that

$$A_t \, B_t^T = -A_\ell \tag{A.3}$$

Solving Eq. (A.3) for B_t^T yields

$$B_t^T = -A_t^{-1} \, A_\ell \tag{A.4}$$

Thus, from Eqs. (A.2) and (A.4) is follows that

$$Q_\ell = A_t^{-1} \, A_\ell \tag{A.5}$$

Using Eq. (A.5), the multiport equations of Eq. (2.1.13) can be rewritten as

$$-\underline{I}_t = A_t^{-1} \, A_\ell \, Y_\ell \, A_\ell^T \, A_t^{-1T} \, \underline{V}_t \tag{A.6}$$

When a Lagrangian measurement tree is selected, it can be shown that

$$A_t = U \tag{A.7}$$

where U is an identity matrix.

Hence, for a Lagrangian measurement tree, the multiport equations are given by

$$-I_t = A_\ell \, Y_\ell \, A_\ell^T \, \underline{V}_t \qquad (A.8)$$

where, the multiport admittance matrix is given by Y_{BUS}.

APPENDIX B. THREE WINDING TRANSFORMER

Let all three winding transformers be represented by the equivalent circuit shown in Fig. B.1a, where

$$a_2 = \frac{N_2}{N_1} \tag{B.1}$$

and

$$a_3 = \frac{N_3}{N_1} \tag{B.2}$$

Three winding transformers can be represented as the three (3) transformer primitive branches shown in Fig. B.1b. Transformer primitive equations are given by

$$\begin{bmatrix} I_1 \\ I_2 \\ I_3 \end{bmatrix} = \frac{1}{y_1 + a_2^2 y_2 + a_3^2 y_3} \begin{bmatrix} -a_2^2 y_1 y_2 - a_3^2 y_1 y_3 & a_2 y_1 y_2 & a_3 y_1 y_3 \\ a_2 y_1 y_2 & -y_1 y_2 - a_3^2 y_2 y_3 & a_2 a_3 y_2 y_3 \\ a_3 y_1 y_3 & a_2 a_3 y_2 y_3 & -y_1 y_3 - a_2^2 y_2 y_3 \end{bmatrix} \begin{bmatrix} V_1 \\ V_2 \\ V_3 \end{bmatrix} \tag{B.3}$$

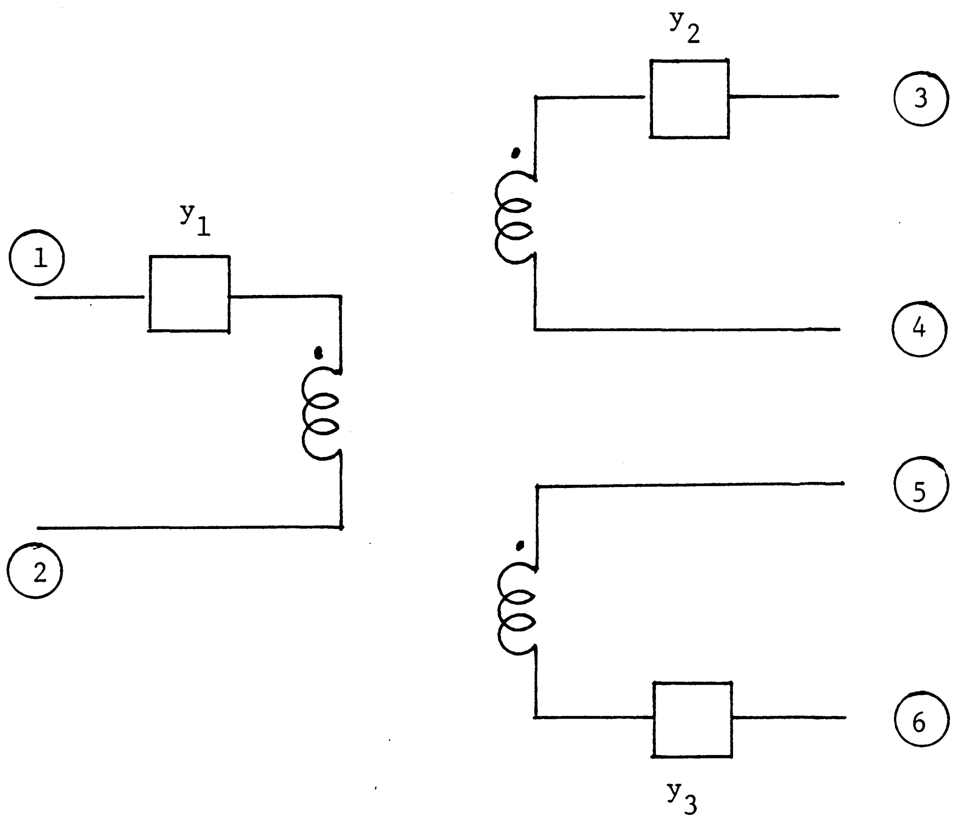

Fig. B.1a. Three winding transformer.

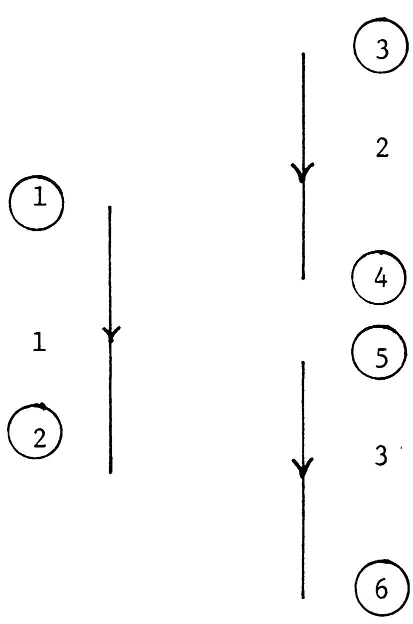

Fig. B.1b. Primitive branches of three winding transformer.

APPENDIX C. TAP-CHANGING TRANSFORMER

Let a single phase tap-changing transformer be represented by the equivalent circuit shown in Fig. C.1a. It can be shown that the ideal auto-transformer contained in Fig. C.1a can be replaced by two linearly dependent sources as shown in Fig. C.1b.

Tap-changing transformer segments can be constructed by the proper interconnection of equivalent circuits. Note that all dependent sources must appear in the system measurement tree. System ports corresponding to these dependent sources must satisfy the following port constraint equations.[34]

$$0 = -I_r + \left[\frac{\bar{a}^* - 1}{\bar{a}^*}\right] I_i \qquad (C.1)$$

$$0 = \left[\frac{\bar{a} - 1}{\bar{a}}\right] V_p + V_{ip} \qquad (C.2)$$

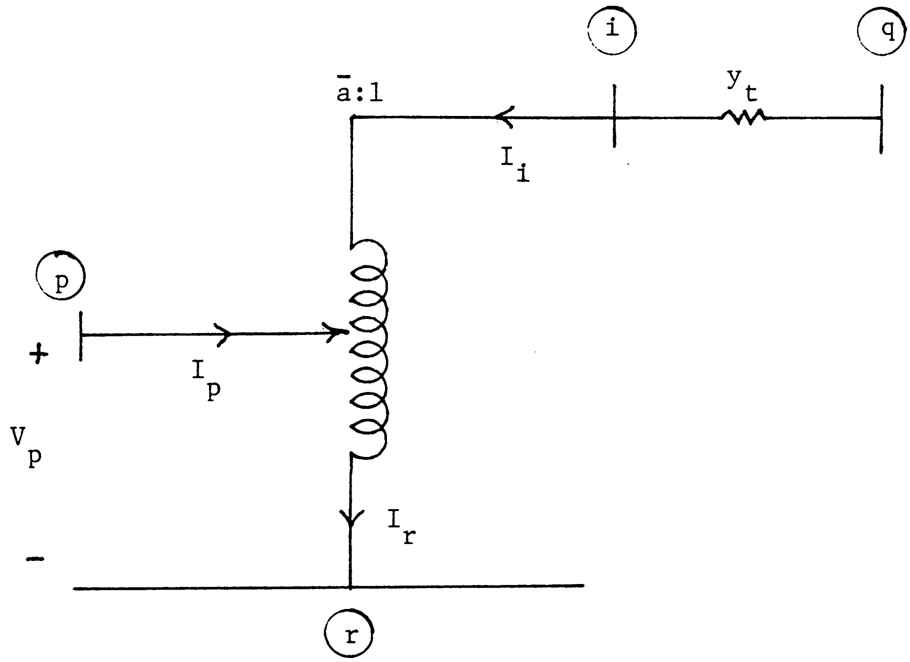

Fig. C.1a. Tap-changing transformer.

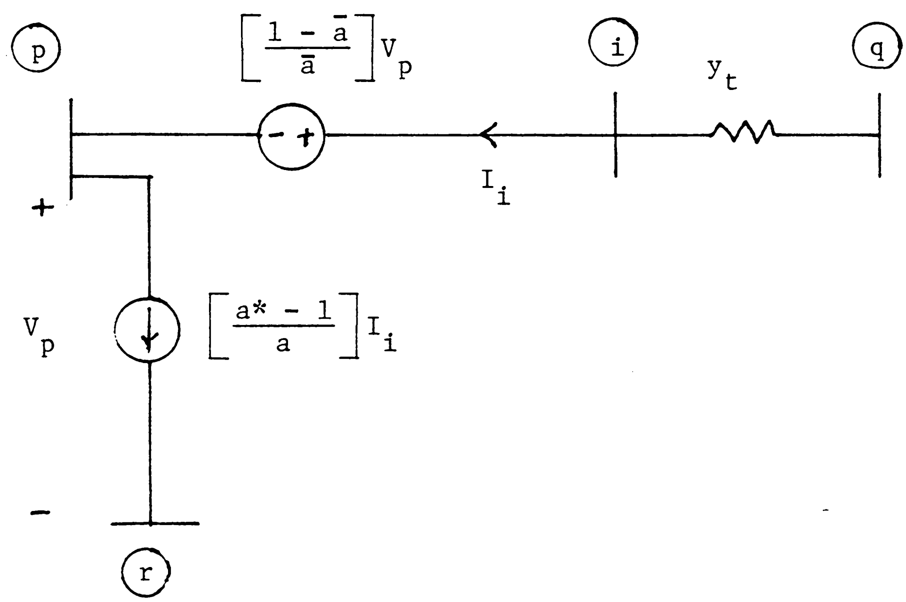

Fig. C.1b. Equivalent circuit for tap-changing transformer.

The vita has been removed from the scanned document

STATE ESTIMATION OF UNBALANCED POWER SYSTEMS

by

Martin A. Wortman

(ABSTRACT)

A new network model has been developed which allows the calculation of state estimates for unbalanced electric power systems. This model incorporates the effects of mutually coupled conductors, earth return paths, unbalanced device configurations, and multiple voltage references.

Development of the new model appeals to multiport network theory and graph theoretic principles. Model equations are employed directly to obtain least squares estimators in the phase-voltage reference frame.

The concept of power system segments is introduced and segment multiport equations are developed. The concept of power system modified primitive networks is introduced and system multiport equations are developed.

Segment and system multiport equations are used to obtain a state estimator formulation in variables suitable for practical systems analysis.